MET O 19 BRANCH MEMORANDUM No.....52.....

THE STRATOSPHERIC SOUNDING UNIT : PERFORMANCE AND PRODUCTS

by

D R Pick and J L Brownscombe

Met O 19
(High Atmosphere Branch)
Meteorological Office
London Road,
BRACKNELL
Berks RG12 2SZ

The Stratospheric Sounding Unit: performance and products

by D R Pick and J L Brownscombe

Table of contents

Summary

The topics covered in this report are the provision and testing programme for the 8 flight models for the TIROS-N series of operational satellites, discussion of the performance of the two flight models now in orbit, retrieval of daily stratospheric charts and assessment of the quality of these products.

Instrumental problem areas highlighted are the greatly increased (but decreasing) noise for channel 27 on TIROS-N (NOAA A SSU is within specification) and the rate of change of gas pressure inside the pressure modulator cells.

Problem areas in the interpretation of results are the relatively large scatter between rocket and satellite measurements (and between different rockets) and retrieval errors under stratospheric warming conditions.

The aim of providing a continuous set of stratospheric analysis for the globe in near real time up to 1 mbar has been met. The r.m.s. difference from conventional analysis is typically less than about 10 dm. A continuous data base should be available from the launch of TIROS-N in October 1978 until the last satellite in the series (1985).

1. Introduction

The Meteorological Office, is providing one of the instruments for each of the recently introduced TIROS-N series of US polar-orbiting operational meteorological satellites. This instrument, the Stratospheric Sounding Unit (SSU), is part of the TIROS Operational Vertical Sounder whose observations have, since March 1979, been used by NOAA to derive the thickness values which form an important input for numerical weather forecasting. In addition to its responsibility for providing these instruments, the High Atmosphere Branch is processing SSU observations routinely to generate thickness and geopotential height analyses for the 100 to 1 mbar region. These stratospheric analyses are being used for research purposes.

The Stratospheric Sounding Unit was first described by Carruthers et al (1973). A further account, which relates the SSU to the other sounding instruments on TIROS-N has been given by Schwalb (1978). Two instruments are now working in orbit, on the satellites designated TIROS-N and NOAA-6 respectively. This report will emphasise the methods being used to generate stratospheric analyses and effects to assess their quality. This is preceeded by a brief accoun of instrumental work since 1976, including a report on in-orbit performance of the SSU.

2. Instrumental Aspects

2.1. Brief description of the Stratospheric Sounding Unit (SSU).

The SSU is a three channel infra-red radiometer, which scans the earth 35° either side of nadir across the orbital track, with a horizontal resolution of 200 km. In-flight radiometric calibration is achieved by periodic views to space & to an internal target, whose temperature is monitored. The pressure modulation technique (Curtis et al, 1974) is used to define the atmospheric weighting functions (the solid curves in figure 1). The different height responses are generated by using different mean pressures of carbon dioxide in the absorption cells which modulate the atmospheric emission in the 15 μm CO_2 band.

Marconi Space and Defence Systems (Frimley) were responsible for the detailed design and manufacture of the Stratospheric Sounding Units under Meteorological Office scientific supervision and project management.

2.2. Provision of SSUs and ground testing programme

The Meteorological Office is committed to providing 8 flight standard instruments. Table 1 gives the instrument construction and delivery schedule. The Development Model was built to confirm the design.

The Protoflight and F2 instruments are in orbit. Three more have been delievered to the USA. The last 3 instruments are in various stages of construction with the last model to be delivered to the USA in mid-1980. Thus, for the later spacescraft in the series, the SSUs will have been assembled for 4 to 5 years prior to launch. As a result, one major cause for concern is stability of the gas content of the modulators and the consequential positions of the weighting functions. This will be discussed later in this section and again in section 3.3.

The ground testing programme can be separated into two overlapping areas. The routine testing, much of which is common to any spacecraft flight instrument, has been carried out by Marconis. The Meteorological Office has used its own test facilities for more detailed radiometric tests, weighting functions measurements and special investigatory tests. The flexibility and expertise of the Office staff are essential in a programme of this type, not only as an independent monitor on the manufacturer but also to enable problems to be investigated quickly without disrupting SSU production.

Both Development and Protoflight models, as a reliability exercise, were subjected to more severe environmental tests than later flight instruments. Modifications in the detailed design, incorporated in the Protoflight as a consequence of the Development Model tests, proved adequate. This testing, as well as the radiometric and weighting function measurements, provided the supporting evidence for the three Design Reviews (Preliminary, Feb 1975; Major, June 1976 and Final, Feb 1977) required by NOAA/NESS and NASA. The Development Model was also used in a preliminary mechanical and thermal test on a simulated spacecraft since, with its freely vibrating pressure modulators and somewhat microphonic detectors, it is sensitive to vibrational interaction. No measurable degradation in SSU performance was found during this test.

Radiometric and angular field of view measurements are made on all complete instruments. The calibration is checked during thermal vacuum testing of the complete spacecraft. All instruments have met the specified requirement for noise (see Table 2). Indeed, for channel 27 which peaks around 1.5 mbar, the noise level has been within the 'design aim' (ie 50% of 'requirement'). The aims of 1K for absolute accuracy in measurement of brightness temperature and 0.5K for interchannel differences (: for scene temperatures between 200K

and 300K) have also been met. Provided a correction is made for a known electrical offset in the space view, the uncertainty in absolute temperature is about ± 0.5K at 200K, decreasing to ± 0.2K at 300K.

Laboratory measurement of weighting functions, which can only be made at the Meteorological Office, have been performed on all individual pressure modulated cells (PMCs) before instrument assembly, and again on all complete instruments. The stability of these weighting functions depends on the constancy of carbon dioxide inside the pressure modulator. The frequency of oscillation and the radiometric calibration constants, all of which can be monitored on the ground and when the instrument is in orbit, only provide an indicator of change of CO_2 pressure within the modulator rather than a direct measurement. The frequency can also vary in response to changes in spring constants or gas mixture, whilst the radiometric constants are also affected by changes in detector and electronic sensitivity and electronic offsets.

It has become apparent that, for all flight instruments, the PMC frequencies are increasing and radiometric calibration constants changing in a way consistent with an increase of gas pressure in the PMCs. When measurements of weighting functions have been repeated, the changes observed have been consistent with an inward air leak. Table 3 shows the magnitude of pressure changes that have occurred to date. These changes are considerably greater than the 10% change in 5 years, which is the worst case design aim, - in the case of protoflight by greater than a factor of 10. The uncertainty in allowing for these changes is in general a more serious source of uncertainty than the uncertainties in systematic radiance errors discussed above. Results since launch are discussed in the next section.

Since leaks into and out-gassing within modulators are obvious dangers, extensive tests on materials were made during the development phase. As a further check, one modulator was put on life test. Over the 2 years of that test, the frequency changed but only by an amount corresponding to a pressure change not exceeding the design aim. Moreover, the frequencies of the two original modulators in the Development Model have shown little change over 4 years . Whilst modifications were introduced in the design of the modulators between the Development Model and the flight instruments, there was no reason to believe that these would affect the stability of pressure. Thus the problem which has emerged is particularly irritating. Since the existing spacecraft and launch programme would involve instruments remaining in air for many years, discussions are underway with the US authorities to seek means of storing the SSUs under more favourable conditions.

2.3. In-orbit monitoring

Data from the Stratospheric Sounding Unit are recorded on board the spacecraft, replayed to one of the two ground stations in the United States and relayed to Suitland, near Washington DC. There the data streams from the various instruments are separated and about half of the raw telemetry data from the SSU is transmitted to Bracknell via a 2400 baud dedicated telecommunications link. These data, which are mainly housekeeping monitors and the radiometer outputs are used to monitor the in flight performance. Figure 2 outlines the monitoring scheme. The output is a mixture of error messages (precipitated by out of limit checks, excessive noise or mirror scan mis-steps) and data prints out and plots over a day or longer. An example of a daily plot is given in Figure 3.

2.3.1. Performance of Protoflight SSU on TIROS N

All housekeeping monitors and two of the three radiometric outputs are operating as expected. The scan mirror is operating correctly and has only lost synchronisation with the spacecraft data system 3 times in 9 months.

Channels 25 and 26 (15mb and 5mb) are consistently performing marginally better than during ground testing, with rms noise ~ 0.3 and 0.5 RU* respectively. Ch 27 (1.5mb) developed a fault during launch (or more precisely before the instrument was switched on in orbit) giving a noise level of $\sim$ 40RU compared with a value in final ground testing of $\sim$ .1 RU. The greatly increased noise is accompanied by a negative offset. It has been possible to duplicate the fault in a number of ways during simulation tests (all involving injecting large noise early in the amplification chain of the signal channel) but the cause of the degradation remains unknown. Both the noise and the negative offset are decreasing

Long term drifts have been found in the PMC frequencies and radiometric calibration constants. The changes seem consistent with a leak of gas from the PMC of about $\frac{1}{2}$ the leak inwards before launch (see Table 3). An orbital variation occurs on some of the housekeeping monitors (see figure 3). This is not reflected in the radiometric calibration, for which spectral analysis shows a variation of less than $\frac{1}{4}$ RU.

---

* 1 RU = 1 mW m^{-2} sr^{-1} $(cm^{-1})^{-1}$

2.3.2. Performance of the F2 SSU on NOAA-6

Since instrument turn-on, on 29 June 1979, all housekeeping and radiometric outputs are operating as expected. The scan mirror is operating correctly and has not yet lost synchronisation with the spacecraft data system (in a period of 2 months). All three radiometric channels are performing consistently, with noise values not worse than those observed during ground testing.

PMC frequencies have changed little since launch compared with the increase observed during ground testing (see Table 3), but radiometric constants have been changing in a similar way to those of the Protoflight radiometer on TIROS-N. This difference in behaviour between the two radiometers makes the interpretation of PMC frequency changes in terms of radiometric and spectroscopic changes more uncertain at present. Comparisons between the two radiometers in the measurement of global mean radiance are planned to provide additional information. The orbital variations in instrument temperature are similar to those shown in Fig 3. However the instrument mounting plate temperature is approximately 5°C colder than on TIROS-N and shows a smaller orbital variation. This has demonstrated the correct functioning of the satellite thermal control system on NOAA-6 compared with the faulty performance on TIROS-N (believed to be due to a thermal control louvre jammed).

3. Weighting Function Aspects

3.1 Calculation and measurement of SSU weighting functions

The weighting functions for the SSU have been computed from instrumental parameters and spectral line data (McClatchey et al 1975) using a line-by-line technique and a Voigt line profile (Drayson 1966). To confirm these calculations, the SSU is used to make laboratory measurements of the transmission of a path through CO_2 at constant pressure (Pick et al, 1976). The result of this comparison is an 'effective mean pressure' (see Table 3), which is the value of mean cell pressure needed to bring the theoretical calculation into agreement with the experimental measurements at a transmission value of 0.5. Difference between filling pressure and effective pressure are caused by outgassing of carbon dioxide and/or leakage of air into the PMC (see 2.2 above). The experimental measurements also show a small systematic shape difference in the transmission against pressure profile (amplitude $\simeq$1% in transmission) compared with the calculation for the effective mean pressure, and this has been included in calculations for the real atmosphere.

3.2 Extrapolation of weighting function to a 'real' atmosphere

The line-by-line calculations are repeated for 19 atmospheres (a sample of representative and extreme atmospheres) at each of the 4 viewing angles and the nadir. These calculations are made for the nominal cell pressure and a cell pressure 10% above nominal. Hence these tables can be interpolated to the mean effective cell pressure and the mean systematic bias removed based on the measurements of Sec 3.1. The technique of McMillin and Fleming (1976 and 1977) is used to interpolate these tables to any arbitrary atmospheric profile. This is repeated for effective pressure + 10%, to quantify the sensitivity of simulated radiance calculations to shifts in weighting function caused by changes in PMC pressure.

A balloon flight was made in March 1976 (Pick & Barwell 1978), in conjunction with NOAA and Oxford University, in which the sun was used as a source of radiation and the atmospheric attenuation was measured with a channel 25 pressure modulator. This tested the above calculations for a measured atmospheric temperature profile from the low troposphere up to 5 mbar. This showed, within the uncertainties of the measurements, that the theory is adequate.

3.3 Comparison with co-located rocketsondes, involving "simulated radiances"

Because of changes in modulator frequencies subsequent to the laboratory measurements of instrumental weighting functions, it is necessary to have an in-orbit check of mean effective pressures. If, at some location, the atmospheric temperature profile has been measured by conventional techniques (ie a rocketsonde), the radiance which the satellite radiometer should observe can be computed from the best estimate of the weighting function. This "simulated radiance" can be compared with the radiance actually observed at the corresponding place and time. An error in weighting function will, dependent on the shape of the temperature profile, cause a difference between the measured and simulated radiances. Indeed, it can be shown that this radiance difference is proportional to the error in mean effective pressure at least over a 10% range in pressure. However any component caused by an instrumental radiometric offset will be independent of the atmospheric temperature structure. Thus these two effects may be discriminated and the mean effective pressure estimated by plotting, for various rocketsonde/satellite comparisons, the difference between measured and simulated radiance against the difference in simulated radiance for a +10% change in mean effective pressure.

Several steps are necessary in matching rocket observations and satellite over-passes to reduce the scatter between them. The basic rocket message is a height temperature profile, which is converted to a pressure temperature profile using a coincident radiosonde ascent or a pressure height analysis. Since the height range of the weighting function exceeds that of the rocket, the rocket profile is extended upwards by a covariance matrix technique based on location and seasonal atmospheric statistics. Spatial and temporal screening is based on the reproducability of the satellite radiance measurements within a search radius of about 200 km around the rocketsonde station. Comparisons are rejected if there is a variation of radiance of more than 3 times the instrument noise within the search radius or a rate of change of radiance of more than 3 times instrument noise per hour. In addition, radiances must be available at times which straddle the rocket measurement. This screening reduces our sample of $\sim$ 1000 rockets from the launch of TIROS-N until February 1979 to about 200.

Two of these were our own Skua rocketsondes, flown from West Geirinish. These flights were launched so as to minimise the time difference between satellite and rocket observations. (A total of nine such flights have been made since the launch of TIROS-N).

For ease of presentation, the differences between measured and simulated radiances have been grouped as station averages; these are shown for channels 25 and 26 of the SSU on TIROS-N in figures 4 and 5.

The main random error in the vertical axis is due to the rocket measurement. Combining an assumed error in the rocket temperature measurement of $\sim$ 1K up to 45 km, increasing to 5 K at 75 km, with the error estimate from the extrapolation technique gives typical uncertainties in simulated radiance equivalent to 1.2K for channel 25, 1.5K for channel 26 (and 2.2K for channel 27). In figures 4 and 5 the scatter about the mean is of this size, the vertical error bars having been reduced by $\sqrt{n}$ (where n is the number of comparisons for the station). The horizontal bars are the actual standard deviation in this parameter.

Several different types of rocketsonde are in use around the world. Figures 4 and 5 show that comparisons involving Russian rocketsondes (from Molodeznaya (stn 1), Volgograd (18) and Heiss Island (27)) are anomolous, the simulated radiances being significantly below the observed radiances. The simulated radiances are computed from the reported temperatures. Comparison flights at Wallops Island of Russian and American sondes, the most recent being in 1977 (Schmidlin, 1978) have revealed biases between them. However, these biases were mainly above 50 km and, in terms of simulated radiance, they correspond to the equivalent of -0.2K for channel 25 and +0.2K for channel 26 compared with US rockets. The mean differences revealed in Fig 4 and 5 are much larger. The results from Wallops Island (16) are significantly different from other sites using the US Datasonde.

For US rocketsondes the mean radiance difference is $0.1 \pm .1$ mW/m^2 sr cm^{-1} for channel 25 and $-0.5 \pm .2$ mW/m^2 sr cm^{-1} for channel 26. These are within our initial uncertainty estimate for absolute measurement by the radiometer. Table 4 illustrates the results of attempting to separate a weighting function shift from a radiance offset. The values deduced are larger than would be expected from ground measurements.

Comparison with rocketsondes will continue, in order to increase the number available (and hence reduce the influence of random errors) and to provide checks on the SSU on NOAA-6. However the present results have raised several questions which we are investigating. In Fig 4 and 5 a systematic latitude effect cannot be separated out, since the station group 4, 8, 9, 10 and 12 are within 20° of the equator while 20 to 24 are around 50°N. This could be an indication of lack of latitude and albedo variation in the rocketsonde short wave correction (Federal Met Handbook #10 (1975) p 1-67). A further complication is the measured diurnal

variation which will cause a systematic difference in radiance for a fixed time difference between rocketsonde flight and satellite overpass.

4. Retrieval of atmospheric thickness

4.1 Basic philosophy

NOAA/NESS are routinely processing data from all channels of the Tiros Operational Vertical Sounder (TOVS) and deducing (and distributing by the Global Telecommunication System) thicknesses for various layers from the surface to 1 mbar. Their retrieval scheme is optimised for the troposphere and lower stratosphere, for which there is a good supply of conventional data (from radiosondes). Their techniques are less appropriate for the upper stratosphere and so it was decided **that a separate retrieval scheme should be developed and run routinely by the High Atmosphere Branch to provide height analyses between 20 and 1 mbar.**

The base pressure level for stratospheric thickness analyses was chosen to be 100 mbar, because this level is well defined by conventional data and analyses are available in association with numerical forecasting models. In practice, in order to have a consistent global base, an analysis produced daily for 1200 GMT by NOAA/NMC is used. Radiances can be derived from the SSU raw telemetry data stream (see Sec 2.3). However, data from other TOVS channels are also needed to cover properly the height range above 100 mbar. Accordingly NOAA/NESS provide us with a second data stream, comprising earth located and calibrated radiances for all the channels shown in Figure 1. This we call the "processed data".

The technique being used to retrieve atmospheric thickness between standard pressure levels from satellite 'brightness temperature' (radiance converted to equivalent black-body temperature) is based on multiple linear regression. This makes use of atmospheric climatological statistics to convert from information measured within the areas of the weighting functions shown in Figure 1 to meteorological parameters at standard levels. In order to derive the regression coefficients, a representative sample of co-located thicknesses and brightness temperatures for all regions and seasons is needed. The normal way of obtaining this sample is to wait until the instrument is in orbit, when directly observed radiances will be available. Because only about 20 rocketsonde profiles become available each week, it would take many months (and perhaps years) to establish a representative sample in this manner. This delay would prevent us from processing the data routinely and promptly.

The approach adopted has been to use an historic catalogue of temperature profiles as the statistical sample and to deduce simulated radiances based on a best estimate of the weighting functions including their temperature dependence. This approach is realistic because of the effort which has been devoted to determining the weighting functions. However, every effort is being made, using the method described in 3.3.above, to verify weighting functions. Whilst the results given in Table 4 seem to indicate a significant error in the weighting functions for TIROS-N, the possibility of systematic latitude effects in rocketsonde/SSU comparisons render the check inconclusive at present. The extent to which the catalogue is representative of the full range of atmospheric conditions is also being studied and is discussed in Sec 5.3 below.

The historic catalogue of temperature profiles used has been carefully compiled by the Upper Air Branch of NOAA/NMC. It contains 1200 different temperature profiles (600 rocket profiles each with two different tie on sondes) with an even spread of summer, winter, polar and tropical profiles. Because of the siting of rocket stations the catalogue is biased towards the northerm hemisphere. The winter profiles include examples of undisturbed and 'sudden stratospheric warming' conditions. This sample forms the basis of the theoretical work in the next section.

4.2. Retrieval techniques and theoretical assessment.

Processed data have only become reliably available since July 1979. Thus a contingency retrieval scheme, based on SSU data only, has had to be used for much longer than expected and thereby acquired greater importance. This section will discuss the performance of various retrieval techniques on the historic sample. But first we must define the measures of performance which have been adopted.

The standard error of estimate (abbreviated as SEE) is the standard deviation of the differences between the actual thicknesses and the thicknesses derived from the regression coefficients and corresponding brightness temperatures. Within this section the SEE is evaluated from the set of thicknesses used to derive the regression coefficients (sometimes called the 'dependent sample'). Whilst this leads to a somewhat optimistic value of SEE, it still gives a good indication of the regression equation's expected performance on an independent sample. Part of the SEE originates in the random noise which

is added to the simulated brightness temperatures prior to the regression analysis, in order to simulate instrumental noise. A similar component arises in the derived thicknesses when the regression equation is applied to an independent sample of observed radiances (which inevitably contain instrumental noise). So long as instrumental noise is random (and not too large) and there is an adequate density of observations, the analysis scheme should effectively suppress these parts of the SEE.

Much more important in operational use are the basic deficiencies of the regression relationship, also expressed by the SEE. The atmospheric temperature structure shows considerable spatial correlation and this is repeated in the radiances. Any limitations in the regression relationship for a particular type of temperature profile will produce an error in thickness over a wide area which cannot be eliminated by the analysis scheme. A common way of reducing this problem is to restrict the range of atmospheric conditions over which the regression equation has to cope. Because of difficulties in recognising which equation must be applied at any time and place, such divisions (often called "zones") are generally defined by latitude and season. Zoning presents its own problems. It will generally introduce artificial discontinuities in derived thickness at the boundaries between zones, which may be overcome by interpolation of coefficients. It also reduces the number of profiles, from within the historic sample, available for regression analysis.

Three regression techniques have been tested: multi-channel regression, step-wise multi-channel regression and principal component regression. In multi-channel regression the derived regression coefficients make use of all of a predetermined set of channels. In step-wise multi-channel regression, data channels are added in order of their partial correlation with the thickness but further addition of data channels is conditional on each producing a statistically significant improvement in the predicted thicknesses. In the principal component method one first computes eigenvectors of the matrix of covariances between the brightness temperatures in the available channels. The channel brightness temperatures corresponding to each temperature profile can then be expressed as a linear combination of these eigenvectors. The coefficients of this linear expansion are used, in place of the individual brightness temperatures, as the 'data channels' for a step-wise regression. A full discussion of the relative merits of these techniques would be out of place here. However, the principal component technique makes more realistic use of highly correlated channels (a common situation with over-lapping weighting functions) and its coefficients generally vary more smoothly

from zone to zone, simplifying any interpolation which may be required.

Retrievals of thickness are being made for the layers 100-20, 100-10, 100-5, 100-2 and 100-1 mbar. It will be obvious that the contingency retrieval scheme, based as it is on SSU data alone with its lowest weighting function centred at 15 mbar, cannot perform well on these layers. The complications of changing the reference pressure surface were not justified for what was deemed a temporary exercise. For much the same reason, our initial retrievals did not use zoned coefficients. The results, for the complete historic sample, are shown in Table 5. As expected, the SEE is high for the 100-20 mbar layer. Much more surprising is the insignificant difference between simulations for TIROS-N and NOAA-6, the former having no data from channel 27. Within the SEE there was a consistent over-estimation of thickness towards low latitudes. Accordingly the historic sample was split into 7 groups:

1) 70°-90° N or S, Winter (ie Oct-March for northern hemisphere);
2) 50°-70°N or S, Winter ;
3) 30°-50°N or S, Winter ;
4) 30°S - 30°N, all seasons;
5) 30° - 50°N or S, Summer (ie April-Sept, northern hemisphere);
6) 50° - 70°N or S, Summer ;
7) 70° - 90°N or S, Summer .

The results for zones 2,4 and 6 are shown in Table 5, again based on SSU data only. Substantial reductions in SEE relative to the unzoned case, are apparent, the improvement being most marked in summer and for 100-20 mbar (the determination of which is most dependent on its meteorological correlation with the upper stratosphere). These improvements are associated with a reduced standard deviation of the sample of thicknesses in all except the winter polar zone (1). Indeed for this zone the SEE is larger than for the un-zoned case. This reflects the wide range of profile shapes which arise from sudden warmings which are somewhat hidden in the global annual sample. For the summer hemisphere and the tropics, values of SEE are between 5 and 8 dm.

Use of the full range of channels available in the processed data-stream (except ch 17, a 4.3 μm HIRS-2 channel, which is known to have a fluorescence problem), leads to the expected improvement in SEE for the lower layers (see Table 6). However, this improvement extends to all levels and zones. The SEE for the summer hemisphere and the tropics is in the range 3-6 dm. Table 6 also provides a comparison between step-wise regression and principal component analysis; the latter without and with channel 27 (ie TIROS-N and NOAA-6). Differences are

subtle and may not be significant. Apart from the total sample and zone 2 (50-70°, Winter), principal component analysis with access to channel 27 provides the lower SEE. However, in the absence of ch 27, multi-channel step-wise regression generally gives a better result.

The rather limited improvements in 100-1 mbar thickness provided by SSU channel 27 stem from this channel's increased sensitivity to the temperature profile above 1 mbar and its larger instrumental noise. However, under stratospheric warming conditions, when the stratopause may drop from ~0.3 to ~10 mbar, the statistics of the temperature profiles are substantially different and the normal regression equations will be in-effective. One would anticipate channel 27 playing a much more important role in regression equations appropriate to these conditions and above all as an indicator of when and where these equations should be applied (see also Sec 5.3).

The principal component regression method, with zoned coefficients, has been adopted for routine use with processed data. Before observed SSU radiances can be used in any regression scheme, corrections must be applied to compensate for the change in height of the weighting function as the radiometer scans away from the nadir. These corrections are also derived from a regression equation, involving the available radiances. Tests indicate that this procedure should not introduce any significant error in the final retrievals.

4.3. Comparison of retrievals with co-located rockets.

Retrievals at 10 mbar and 20 mbar have been assessed as analysed products; these are discussed in section 5.3. Above 10 mbar co-located rockets provide the basis for comparison. Differences between the height of the standard constant pressure levels derived from the rocket measured temperature profile and by regression from co-located measured satellite radiances, can be attributed to poor spatial and temporal co-location, to the statistical nature of the retrieval scheme and to errors in weighting functions. The co-location criterion used here is not as elaborate as in section 3.3. Table 7(a) lists the 100-1 mbar thickness comparison; it is apparent that the standard deviation is much more sensitive to changes in the distance than in the time difference used in the co-location procedure. Further subjective screening, to exclude measurements under tight gradient or rapidly changing situations, results in figure 6. Also included in figure 6 is the performance of the two channel retrieval scheme on the historic sample used to generate the regression

coefficients. This figure shows we are close to the theoretical limit of the retrieval scheme. This figure also does not support the shift in weighting function estimated in table 4. Such a weighting function error corresponds to an expected bias of 30 dm in the 100-1 mbar thickness, compared to the observed bias of 8 dm. Similar work has been done on the lower levels and is summarised in Table 7(b).

5. Analysis and comparison of charts

5.1. Interpolation and smoothing techniques

The spacing between individual observations is approximately 200 km, the eight observations in each SSU scan line providing a swath 1400 km wide centred on the sub-satellite track. Gaps in coverage occur between successive orbits at latitudes below $\sim 40^{\circ}$, but over a 24 hr period these gaps generally get filled except near the equator. However, other gaps in coverage may arise because sections of the data are lost. Most frequently such gaps comprise a complete orbit.

For many purposes (eg for producing charts or for quantitative dynamical studies) it is useful to represent the data by a set (or grid) of values at known fixed geographical locations, or in terms of the coefficients of spatial patterns. In either case, the analysis procedures reduce the number of values needed to represent the state of the atmosphere. Two types of grid are in use for SSU products : a polar stereographic projection with a grid length of 250 km at 50°, which is used poleward of latitude $\sim 15^{\circ}$, and a rectangular latitude/longitude grid with 5° ($\simeq$550 km) spacing.

In order to interpolate to the grid points, each observation within a specified search radius and a specified time window is weighted with respect to its distance from the grid point and the time interval between the observation and analysis time. The weighting function used at present for distance is a simple 'conical' scheme, ranging from 0.0 at the boundary to 1.0 at the centre. Similarly, the time weighting function is triangular, increasing linearly from 0.0 at both edges of the time window to 1.0 at the analysis time. The distance and time components are multiplied to give an overall weighting, and the grid point value is then derived from the sum of all the selected observations.

Background data can also be included if required. Values normally used for the search radius and time window are 500 km and (plus/minus) 12 hours respectively. When data from the two spacecraft are merged, these values will be changed to 300 km and 6 hours. Smoothing is carried out in two stages. First, any grid points with no observations (eg because of a missing orbit) are given values based on linear interpolation between the nearest 'good' data east and west of the missing point. Second, the entire field is smoothed by the method of orthogonal polynomial fitting in 2-dimensions. In the case of the global field, the 'orthogonal polynomials' are orthogonal fourier coefficients. The fitting normally used is order 12 for the polynomials, and 10 wavenumbers for the fourier coefficients. Fig.7 provides examples of the variations of the coefficients with order for a chart with high amplitudes at wavenumbers 1 and 2. The truncation limits, quoted above, are conservative.

5.2. Multiple analysis scheme

In an attempt to exploit the theoretical improvement in quality of retrievals from processed data, compared with retrievals from two channel SSU data on TIROS-N, and cope with erratic reception of processed data, a multiple analysis scheme has been developed.

This scheme is outlined in Figure 8. The essentially complete coverage of retrievals from SSU data are analysed to produce a background field for analysis of the often in-complete coverage of retrievals from processed data. This latter analysis is done twice, because the extra smoothing used in the first analysis (in order to suppress the edge-effects caused by missing data) attenuated highs and lows. Experience with this scheme, applied to data from the northern hemisphere, showed a significant improvement in quality over previous charts. The scheme is currently in routine use, whilst the problems in receiving complete processed data are being resolved.

5.3. Comparison of analyses with conventional measurements

Since analyses are the end-product which will be most used, it is important that they should be validated. Whilst this stage of validation ought to concentrate on the analysis procedures, it also serves to high-light residual retrieval problems and identify the synoptic situations in which they occur. To date the majority of comparisons have been made for analyses of 2-channel SSU data, retrieved with either zoned or un-zoned coefficients. Whilst these analyses are expected to be worse than those retrieved from

processed data, the exercise has proved worthwhile by causing us to set up the necessary comparison techniques and gain experience in the interpretation of the results.

For several years charts up to 10 mbar have been produced in the High Atmosphere Branch based on radiosonde, and occasional rocketsonde, observations using manual techniques exploiting continuity. We believe that the quality of these charts, produced in retrospect under research conditions, is such that they may reasonably be used as a standard against which the satellite analyses may be compared. However, such comparisons must take account of the differing horizontal and vertical resolution of the observational techniques and the asynoptic nature of the satellite data. Charts for the 10 and 20 mbar levels have been used in comparisons with SSU analyses.

In general, at 10 and 20 mbar both sets of charts showed similar flow patterns. The locations of highs and lows were usually closely similar, except in mobile situations when the SSU charts smeared features. This was principally a result of time differences between the observations being used. Of course, there was another cause for smearing of features in the satellite charts which arose from interaction between the broad vertical resolution of the satellite observations and the westward tilt of chart features with height. It was also noticed that the normal uniform geopotential height at the centre of highs was not so well represented in SSU analyses and that, with lows, gradients in the fields were too evenly distributed. These resulted from a combined analysis and retrieval problem. Later in the winter features appeared on the SSU charts some days before they became evident on the hand drawn charts. This effect was usually associated with a period of warming where the upper part of the weighting functions were responding to the warmer higher layers. This disturbance was being 'propogated' down by the regression coefficients. Chart comparisons also revealed an equatorward bias, of 10-12 dm, in the satellite charts which was alleviated by the use of zoned regression coefficients. Table 8 presents some differences between satellite analyses and the hand-drawn charts relating to the centres of lows and highs and a pair of geographical locations which provide a measure of the latitudinal gradient. The general improvement resulting from the use of processed data should be noted. The exception, in the centre of lows, is being investigated.

Objective chart comparisons, in the form of difference charts and difference statistics, high-lighted further problems. Areas of maximum disagreement (up to 100 dm) were found near sharp gradients. A small discrepancy in the shape

or direction of a jet axis for instance produces large local differences. There are several processes which could cause these differences : retrieval error; motion of features which can change both gradients and shapes of features; evolution of features within the analysis period and smoothing of fields introduced to suppress noise. There are instances where any of these processes could be seen to apply, either singly or in conjunction. When extended areas of large differences were examined, it was often found that they corresponded with areas where the temperature profile could be expected to be anomolous in some sense, for instance during the evolution of a warming. In these areas the usual atmospheric correlations would not apply and the regression equations used to estimate the temperature would be inappropriate; this would be especially severe for the two channel SSU retrievals. This is something which will possibly improve now that the topmost SSU channel is available on NOAA-6. However, it is a problem which should certainly be further investigated. It might be beneficial to use locally varying regression equations which can compensate for the 'non-statistical' character of a small region. The difficulty may be to determine such areas from the satellite radiances.

Table 9 provides some statistics concerning the mean difference between charts, whilst Figure 9 shows the appropriate charts for 4 Jan 1979. The warm error pool (for the satellite) near 60°N and 140°E is a typical retrieval problem area of the type described above.

Table 10 shows some of the results of comparing rocket measured profiles with values interpolated from the appropriate satellite-based analyses. For this table, two sites have been chosen which show large atmospheric variance during the period 16 December 1978 to 7 May 1979. The variance of the height of the pressure levels 5,2 and 1 mbar are similar for the rocket ascents, the site values extracted from the charts and the rocket catalogue profiles used for calculating the regression coefficients. This gives confidence in the representativeness of the rocket catalogue used in calculating the regression coefficients, and demonstrates that the satellite charts are responding adequately to different atmospheres.

However, the standard deviation of the difference between the height derived from the rocket measurement and the height extracted from the appropriate chart is larger than the expected standard error of estimate evaluated when calculating the appropriate regression coefficients. This difference can be accounted for by including a contribution to the standard deviation derived

from the comparison of the measured satellite radiance and the simulated radiance from the rocket profile. This radiance 'noise' is converted to an equivalent height 'noise' using the appropriate radiance to height regression coefficients. In practice this term dominates the component arising from the standard error of estimate of the retrieval.

The differences between simulated radiances and observed radiances, which were also seen in Sec 3.3, probably arise from the different spatial scales sampled by the rocketsonde and satellite observations. These real differences suggest that it would be unwise to force satellite analyses to conform to the few available rocketsonde observations.

6. Products

Data are received from Washington on an orbit by orbit basis and recorded on magnetic tape. The tape is dis-mounted at about 1700 GMT each day and data for a 24 hour period centred on 12 GMT of the previous day is processed overnight on COSMOS. (At an earlier stage the analysis was for the 24 hours centred on 00 GMT, but delays in receiving the processed data have caused us to make this change). An outline of the total processing scheme is given in Figure 10. More details of the instrument monitoring and stratospheric analysis schemes have already been given, in Figures 2 and 8. These procedures have proved effective and robust. Nearly all data received have been processed, although naturally the quality of products has improved with time. Wide use is made of the Calcomp 1670 to generate output on 35 mm film, from which A4-size prints are subsequently obtained by a dry-silver process. An example, associated with instrument monitoring, was given in Figure 3. Another very important chart (Figures 11a and b) indicates those sections of the sub-satellite track from which data have been received. This chart is often useful in assessing the confidence which may be attached to features in the stratospheric analyses. For economy and convenience the analyses in polar stereo-graphic projection are drawn on a scale which allows 6 charts to be presented on a single 35 mm frame. Various analyses are coded and output on punched paper tape, for transmission by telex.

It is essential that there is access to digital data for quantitative studies of the analyses (both within and outside the Office), for generation of plots of instrument performance etc. over extended periods and for further development of the processing scheme. Thus the raw data received from Washington, the final analyses and a wide range of intermediate and ancillary products are being archived on magnetic tape. A list of the products, identifying those which are archived, is given in Annex A. We are collating the charts (eg Fig 9 and 11-14 below) into book form, which can be purchased, as a guide to the digital data.

Examples of some of the chart outputs for 1 July 1979 (ie the first day after the switch-on of the SSU on NOAA-6) are provided: southern hemisphere radiances, Fig 12; southern hemisphere thicknesses, Fig 13 and northern hemisphere geopotential heights, Fig 14. In Figures 12 and 13 results from TIROS-N and NOAA-6 are shown, in a) and b). At this stage data from the two spacecraft were being treated separately. The charts demonstrate that the reproducability between the two Stratospheric Sounding Units is better than $1^{\circ}K$ in equivalent

brightness temperature. Differences between the thickness charts (Fig 13) are primarily the result of the data channels used in the retrievals: processed data (from HIRS/2, MSU and SSU) for TIROS-N but SSU (3 channel) data for NOAA-6. For the 100 - 1 mb thickness, the values at the centre of the polar vortex agree to within 8 dm.

7. Use of the products

The objective in producing stratospheric analyses is to improve understanding of the behaviour of the stratosphere and its dynamical processes, and their influence on minor constituents and inter-actions with the rest of the atmosphere. In these contexts, the products which have been described in this paper will allow studies originated with data from the Oxford/Heriot-Watt Selective Chopper Radiometers to be continued and extended. Whilst it is probable that many of these research activities will be beyond the bounds of the High Atmosphere Branch, it is appropriate that some dynamical studies are conducted within the group responsible for generation of the products. In this way limitations of the products are exposed and incentives for improvement are reinforced. Thus, despite the known limitations of the analyses, a study of dynamical developments during the 78/79 winter has been undertaken. With improvements in retrieval schemes and the availability of data from two satellites, more elaborate and convincing studies will be possible for the coming winter. Another use of the data has been to check recent predictions of the diurnal variation of stratospheric temperature.

It is encouraging that products have already been requested by several groups in the UK and abroad. Charts are sent regularly to Professor Labitzke (Free University, Berlin) for use in her studies of stratospheric climatology. During the winter, radiance analyses were sent daily by telex to assist them in their stratospheric analysis and in the generation of Stratalert messages. Charts are exchanged with the Upper Air Branch of NOAA/NMC (Mr Finger), for comparison with similar analysis which they are producing based on SSU and rocketsonde data. Data is sent weekly by telex to Dr Khodkin (Moscow) for use in conjunction with their rocket measurements. British Aerospace have been provided with data in connection with studies of Concorde sonic booms. Dr Barnett (Oxford University) has used our data in conjunction with interpretation of observations from their SAMS experiment on Nimbus 7. Dr Harwood (Edinburgh) and Professor Hirota (Kyoto University) have requested data for their studies of stratospheric dynamics and Professor Dütsch (Zurich) is using our products in some studies of atmospheric ozone. In several cases (ie Oxford, Berlin, NOAA/NMC) there has

already been useful feedback leading to improvements in our processing scheme.

8. Future programme

It will be apparent that there are many tasks yet to be completed and others still awaiting attention. It is only possible to mention some of them.

On the instrument side, Marconis should deliver the last three radiometers by mid-1980, but integration and testing of instruments with spacecraft will continue beyond that date. Further laboratory measurements of weighting functions are planned, to substantiate theoretical estimates of the effects of variations in gas composition within the modulator and of the dependence of weighting functions on temperature.

The whole question of monitoring the weighting functions in orbit and particularly the interpretation of radiance comparisons with rocketsondes (Sec 3.3) remains to be resolved. The possibility of using global mean radiances, to study temporal changes of weighting functions and differences between instruments, will be investigated.

Further detailed investigations of retrievals from processed data are required and a special effort will be made to find a workable method of improving retrievals under warming conditions. The effects of retrieval errors on dynamical studies will be investigated. Various schemes for merging data from two satellites, observing at different local times, must be evaluated and consideration given to ways in which conventional data (e.g. rocketsondes) might be directly incorporated into the analyses.

9. Conclusions

Since the interim report in January 1976 (MRCP 393) the instrument programme has progressed to the stage where two Stratospheric Sounding Units are operating satisfactorily and reliably in orbit. Data from these instruments is being used by NOAA in their operational temperature retrievals for the troposphere and stratosphere. A processing scheme has been developed which allows stratospheric data, received at Bracknell, to be handled routinely and our obligations, to monitor instrument performance and produce daily stratospheric analyses up to the 1 mbar level, to be met. The quality of these analyses is already quite high but means for further improvement are being investigated. These are substantial achievements. As the preceding section has shown, there are some problem areas (but we believe none which are really serious) and much still to be done. There is every indication that the series of Stratospheric Sounding Units will provide an effective means of routinely observing the stratosphere into the mid-1980's. The stratospheric analyses should be an important element in the interpretation of observations of minor constituents, by instruments on Nimbus-7 (eg the Oxford SAMS experiment) and other planned satellites, and also contribute to the understanding of dynamical processes and their representation in numerical models of the stratosphere.

Acknowledgements

This paper records the outcome of the efforts of past and present members of the SSU instrumentation and stratospheric analysis groups of Met O 19. Text has been supplied by H J Baker, J S Campbell, I S Cook, M Needham, J Nash and T N Palmer. G P Carruthers, B Tonkinson and G C Bridge have been responsible for SSU project management. Continuing co-operation of Met O 5 and Met O 12 is essential to the smooth running of the data processing. We acknowledge the work of those responsible at MSDS Ltd (Frimley) for SSU design, construction and testing and those staff of NOAA/NESS, NASA and RCA who have been involved with the Stratospheric Sounding Unit.

References

Carruthers G P, May B R, Miller D E and Stewart K H. 1973
Some current work on meteorological satellites.
Meteorological Magazine 102 pp 258-265.

Curtis P P, Houghton J T, Peskett G D, and Rodgers C D. 1974.
Remote sounding of atmospheric temperature from satellites V. The pressure modulator radiometer for Nimbus-F.
Proc R Soc Lond A 337 pp 135-150.

Drayson S R. 1966.
Atmospheric transmission in the CO_2 bands between 12 μm and 18 μm.
App Optics 5 pp 385-391.

Federal Meteorological Handbook Number 10. 1975.
NASA, US Dept of Commerce and US Dept of Defence.

McClatchey R A. 1975.
Data described in McClatchey R A, Benedict W A, Clough S A, Burch D E, Calfee R F, Fox K, Rothman L S, and Garing J S. 1973.
AFCRL Atmospheric Absorption Line Parameters Compilation.
AFCRL TR 730096.

McMillin L M and Fleming H E. 1976.
Atmospheric transmittance of an absorbing gas: a computationally fast and accurate transmittance model for absorbing gases with constant mixing ratios in inhomogeneous atmospheres.
App Optics 15 pp 358-363.

McMillin L M and Fleming H E. 1977.
Atmospheric transmittance of an absorbing gas. 2: A computationally fast and accurate transmittance model for slant paths at different zenith angles.
App Optics 16 pp 1366-1370.

Pick D R, and Barwell B R. 1978.
Analysis of the balloon flight of 17 March 1976 which measured atmospheric transmission using a pressure modulator equivalent to the high pressure channel of the Meteorological Office Stratospheric Sounding Unit.
Met O 19 Branch Memorandum 45.

Pick D R, Warner D E, Kent P and Carter R D. 1976.
Stratospheric Sounding Unit (SSU) for TIROS-N: Radiometric and Spectroscopic Performance of the D1 Development Model.
SSU Technical Communication No 98.

Schmidlin F J. 1978.
Results of the US-USSR meteorological rocketsonde intercomparison held at Wallops Island, Va, August 1977.
WG6, COSPAR XXI, Innsbruck.

Schwalb A. 1978.
The Tiros-N/NOAA A-G Satellite series.
NOAA Technical Memorandum NESS 95.

TABLE 1 Programme of Provision of SSUs

Instrument / Activity	Development Model	Protoflight.	F.2	F.3	F.4	F.5	F.6	F.7	F.8
Instrument completely assembled	June 76	Nov 76	Feb 77	May 77	July 77	April 78	Dec 79?	Oct 79	March 80?
Delivered to Meteorological Office	Sept 76	Jan 77	May 77	Aug 77	Oct 77	June 78	March 80?	Jan 80?	July 80?
Delivered to USA		March 77	Aug 77	May 78 Feb 79*	April 78 June 78*	June 79	May 80?	Jan 80?	July 80?
Integrated with spacecraft		June 77	Oct 77	June 78 May 79*	Jan 79	?	?	?	?
Launch: - date		13 Oct 78	27 June 79	June 81?	Oct 80?	Oct 82?	Oct 84?	June 83?	June 85?
- satellite		TIROS-N	NOAA-6						

* After re-work

? Planned dates (Launch dates assume 2 year spacecraft lifetime)

TABLE 2 Radiometric performance of SSUs.

	Specified "Requirement"	Measured Values for complete instruments Protoflight	F.2.	F.3.	F.4.	F.5.
TOVS channel 25 Nominal height 15 mbar (29 km)						
a) Noise in RU	0.375	0.35 (0.3) *	0.3 (0.3)*	0.35	0.3	0.25
b) Noise in K						
at i) 300K	0.25	0.25	0.2	0.25	0.2	0.15
ii) 200K	0.5	0.5	0.4	0.5	0.4	0.4
TOVS Channel 26 Nominal height 5 mbar (37 km)						
a) Noise in RU	0.75	0.5 (0.5)*	0.5 (0.4)*	0.4	0.3	0.3
b) Noise in K						
at i) 300K	0.5	0.35	0.35	0.25	0.2	0.2
ii) 200K	1.0	0.7	0.7	0.55	0.4	0.4
TOVS Channel 27 Nominal height 1.5 mbar (45 km)						
a) Noise in RU	1.875	0.9 (40)*	0.6 (0.6)*	0.6	0.6	0.95
b) Noise in K						
at i) 300K	1.2	0.5	0.4	0.4	0.4	0.6
ii) 200 K	2.4	1.0	0.75	0.75	0.75	1.2

1 RU = 1 mW m^{-2} $sr^{-1}(cm^{-1})^{-1}$

* in-orbit value soon after launch-TIROS N channel 27 had improved to 12 RU by Oct. 1979.

TABLE 3 PMC PRESSURE CHANGES

TOVS CH No.	Nominal filling pressure (mbar)	Po (WF) (mbar)			TIROS-N P/F	NOAA-6 F2	NOAA-C F3	NOAA-B F4	NOAA-D F5
25	108 @ 30°C	106.0 ± 1.	$\Delta p(f)$	mbar	8.0	4.4	3.6	5.8	7.4
			dp/dt(air),	mbar/100 days	1.0	0.6	0.4	0.6	1.0
			$\Delta p(WF)/\Delta p(f)$		-	-	-	-	-
26	35.6 @ 30°C	37.1 ± 0.7	$\Delta p/f)$	mbar	9.3	5.2	6.2	5.1	4.6
			dp/dt(air),	mbar/100 days	1.1	0.6	0.7	0.6	0.65
			$\Delta p(WF)/\Delta p(f)$		0.7 ± 0.2	0.9 ± 0.5	0.4 ± 0.2	0.2 ± 0.3	0.4 ± 0.2
27	10.8 @ 30°C	11.0 ± 0.15	$\Delta p(f)$	mbar	7.9	4.5	6.7	3.3	3.0
			dp/dt(air),	mbar/100 days	1.0	0.5	0.5	0.5	0.5
			$\Delta p(WF)/\Delta p(f)$		0.7 ± 0.2	0.6 ± 0.2	0.4 ± 0.1	0.3 ± 0.2	$0.4^{+} - 0.1$

For P/F and F2 Δp is from the time at which the PMC was finally sealed until Launch

For F3,F4,F5 Δp is from the time at which the PMC was finally sealed until 10 August 1979.

$\Delta p(f)$ is the pressure change implied from frequency change assuming no change in the mechanical performance of the PMC.

$\Delta p(WF)$ is the effective CO_2 pressure change as measured in weighting function tests at the Met Office.

p_o (WF) is the average of the effective mean CO_2 pressure as measured in weighting function tests at the Met Office immediately after final sealing of the PMCs.

Channel	PMC pressure shift	radiometric offset mW/m^2 sr cm^{-1}	standard deviation mW/m^2sr cm^{-1}
25	$+ 10 \pm 3\%$	$.8 \pm .2$	1.2
26	$+ 15 \pm 4\%$	$1.0 \pm .5$	2.3

TABLE 4. Changes to SSU weighting functions and radiometric offsets required to bring radiances observed by SSU on TIROS-N into agreement (on average) with simulated radiances derived from co-located rocketsondes (excluding Russian rocketsondes). These changes assume no residual systematic errors in the rocketsonde measurements. All data shown in Fig 4 and 5, covering the period Oct 1978 - Feb 1979, have been used. The quoted standard deviations are computed about the best-fit lines shown in the figures.

TABLE 5. Retrieval statistics for multi-channel step-wise regression on SSU data only and the historic sample of ascents. Firstly un-zoned, then for 3 of 7 zones.

Layer mbar	Standard Deviation of sample: thickness dm	temperature °K	size of sample	Standard Error of Estimate dm Tiros-N	NOAA-6
Unzoned					
100 - 20	36.5	7.7	1200	15.5	14.3
100 - 10	50.2	7.4		11.3	11.0
100 - 5	68.2	7.8		7.6	8.1
100 - 2	97.9	8.5		8.7	8.9
100 - 1	121.7	9.0		13.0	12.2
Zone 2	50-70° latitude winter				
100 - 20	38.1	8.1	213	11.0	9.5
100 - 10	55.1	8.2		9.1	8.7
100 - 5	70.2	8.0		6.9	7.3
100 - 2	88.0	7.7		9.3	8.6
100 - 1	102.0	7.6		13.5	13.2
Zone 4	30°S-30°N, all seasons				
100 - 20	13.5	2.9	400	8.0	8.1
100 - 10	17.4	2.6		7.1	7.1
100 - 5	23.1	2.6		6.4	6.1
100 - 2	30.9	2.7		6.7	6.3
100 - 1	34.9	2.6		6.9	7.0
Zone 6	50-70° latitude, summer				
100 - 20	17.3	3.7	202	5.4	5.5
100 - 10	29.7	4.4		5.5	5.6
100 - 5	44.7	5.1		5.0	4.6
100 - 2	65.0	5.7		4.8	4.3
100 - 1	76.1	5.6		5.1	5.1

TABLE 6. Retrieval statistics for retrievals from processed data. For Tiros-N: method A, step-wise regression; method B, principal component regression. For NOAA-6: method B, principal component regression.

Layer mbar	Standard Deviation of sample: thickness dm	temperature °K	size of sample	Standard Error of Estimate, dm Tiros-N method A	Tiros-N method B	NOAA-6 method B
Unzoned						
100 - 20	36.5	7.7	1200	3.8	4.3	4.7
100 - 10	50.2	7.4		4.6	4.9	6.2
100 - 5	68.2	7.8		5.4	5.8	5.5
100 - 2	97.9	8.5		6.2	7.4	7.0
100 - 1	121.7	9.0		8.8	9.0	10.2
Zone 2	50-70° latitude, winter					
100 - 20	38.1	8.1	213	3.7	4.6	5.1
100 - 10	55.1	8.2		5.0	5.1	6.8
100 - 5	70.2	8.0		6.5	6.2	6.8
100 - 2	88.0	7.7		8.0	9.2	8.4
100 - 1	102.0	7.6		11.0	11.7	12.9
Zone 4	30°S-30°N, all seasons					
100 - 20	13.5	2.9	400	3.0	3.0	2.9
100 - 10	17.4	2.6		3.2	3.2	3.0
100 - 5	23.1	2.6		3.9	3.8	3.3
100 - 2	30.9	2.7		4.5	4.5	4.0
100 - 1	34.9	2.6		4.8	4.8	4.5
Zone 6	50°-70° latitude, summer					
100 - 20	17.3	3.7	202	2.7	2.9	2.8
100 - 10	29.7	4.4		3.5	3.7	3.5
100 - 5	44.7	5.1		3.9	4.0	3.4
100 - 2	65.0	5.7		4.4	4.6	3.9
100 - 1	76.1	5.6		4.8	4.7	4.7

TABLE 7

Comparison of rocket measured thickness and satellite derived thickness calculated, using two channel zoned regression coefficients, from TIROS-N SSU data. (Differences and standard deviations in dm).

a) 100 - 1 mbar thickness data

Distance of co-location from rocket site	Time from rocket launch ± 3 hrs			± 6 hrs			± 12 hrs		
	mean diff	standard deviation	No of obs	mean diff	standard deviation	No of obs	mean diff	standard deviation	No of obs
≤ 75 km	-6.0	26.7	15	8.0	32.9	29	6.3	31.9	48
≤ 125 km	1.0	28.8	44	4.9	28.4	79	3.3	26.5	136
≤200 km	-1.3	52.4	101	1.0	46.0	184	2.5	42.1	268

b) all standard levels derived: co-location distance ≤125 km, time ± 12 hrs

levels mbar	mean diff	standard deviation	number of observations
100 - 20	-2.7	12.4	136
100 - 10	-3.6	12.8	136
100 - 5	-3.9	14.8	136
100 - 2	-1.7	20.8	136
100 - 1	3.3	26.5	136

TABLE 8

Spot comparisons between satellite analyses, based on SSU data and processed data respectively, and hand analyses of radiosondedata.

Differences in Decametres.

20 mbar	At centres of:				At geographical locations:			
	LOW		HIGH		90°N,0°W		30°N, 0°W	
	mean	SD	Mean	SD	mean	SD	mean	SD
SSU data-hand drawn	8.0	6.2	1.8	17.2	-8.9	20.2	18.3	8.7
Processed data-hand drawn	15.3	6.7	-0.3	5.3	-4.2	13.6	8.3	7.7
10 mbar								
SSU data-hand drawn	15.2	7.4	8.7	20.4	17.6	33.7	22.9	6.4
Processed - hand drawn	19.4	6.1	2.8	11.7	9.3	19.4	11.4	8.1

These comparisons were made on all Thursdays (9) when both PROCESSED and SSU charts were available to compare with hand drawn charts.

TABLE 9

Objective comparison between charts produced by hand analysis of radiosonde data at 10 mbar and 20 mbar and charts derived objectively from satellite data. The mean and standard deviation have been evaluated for grid points corresponding to the Met Office octagon system. The satellite charts have been derived from SSU channels only, called 'SSU' (using un-zoned coefficients) or from HIRS, MSU and SSU channels, called 'processed'.

Date	pressure level, mbar	Processed charts - hand drawn charts		SSU charts - hand drawn charts	
		mean, dm	standard deviation	mean, dm	standard deviation.
4.1.79	20	7.6	11.6	18.7	16.9
8.2.79	20	1.5	11.3	13.8	18.8
15.2.79	20	3.9	8.7	16.1	13.2
19.4.79	20	4.9	8.1	15.7	16.8
4.1.79	10	9.5	12.0	20.9	15.1
8.2.79	10	6.2	13.0	17.2	17.4
15.2.79	10	7.0	10.7	18.1	14.2
19.4.79	10	9.1	10.3	19.8	14.2

TABLE 10

Examples of the comparison between heights of constant pressure surfaces extracted from the satellite charts (based on 2 channel SSU data with unzoned coefficients) and heights derived from rocket sonde temperature measurements. The two sites shown have large atmospheric variance between 16.12.1978 and 7.5.1979.

Pressure level mbar	Derived height field, dm: rockets SD	Charts on same days SD	Charts - Rockets: mean	Charts - Rockets: SD
For Thule (for 19 ascents)				
20	62 (36)[2]	49	2	18 (15)[1]
10	74 (50)	63	4	15 (12)
5	86 (68)	77	7	17 (30)
2	103 (98)	92	11	24 (25)
1	113 (122)	104	12	26 (26)
For Chatanika (for 32 ascents)				
20	58 (36)[2]	62	-8	12(15)[1]
10	83 (50)	84	-2	11 (12)
5	92 (68)	104	-10	20 (19)
2	114 (98)	125	-18	22 (16)
1	126 (122)	137	-32	27 (22)

Channel number, SSU	Radiance fields, mw/(m^2 sr cm^{-1})			
for Thule				
26	7.9	7.5	1.0	1.7
25	8.0	7.0	1.2	2.5
For Chatanika				
26	8.8	8.8	-0.2	0.9
25	9.3	9.2	-1.2	1.4

Notes. SD = standard deviation for the sample

Note 1. The quantity in brackets is the estimated standard deviation derived by combining the expected retrieval error (standard error of estimate) and the height error due to the difference between simulated radiance from the rocket profile and the satellite radiance. The largest contribution to this term is the variance between the satellite measured radiance and the simulated radiance calculated from the rocket profile.

Note.2. The quantity in the bracket is the standard deviation derived from the catalogued rocket sample used to calculate the regression coefficients.

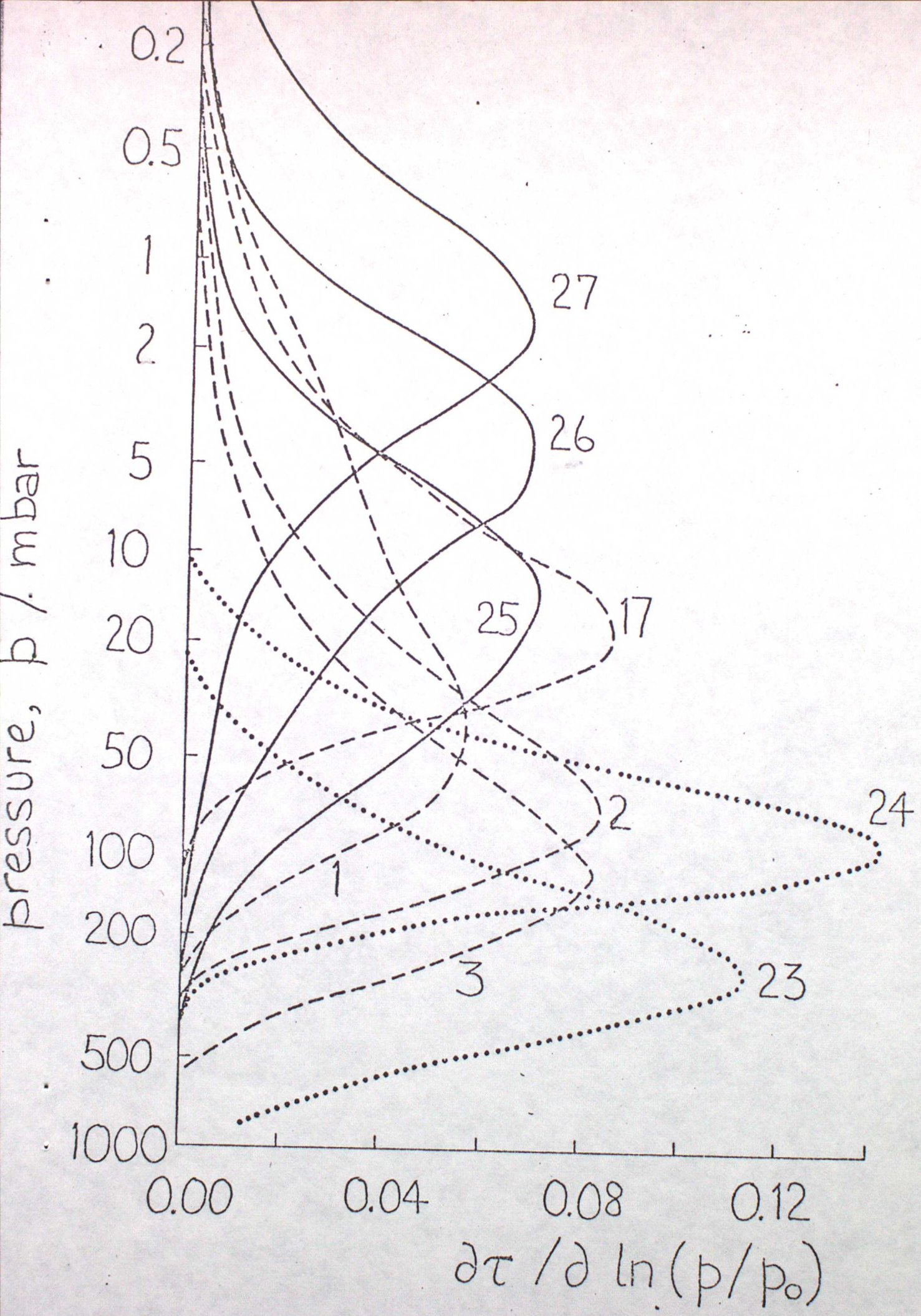

FIGURE 1. Weighting functions for those channels of the Tiros Operational Vertical Sounder which are relevant for the stratosphere. Curves are labelled with their channel number.
———, channels of Stratospheric Sounding Unit.

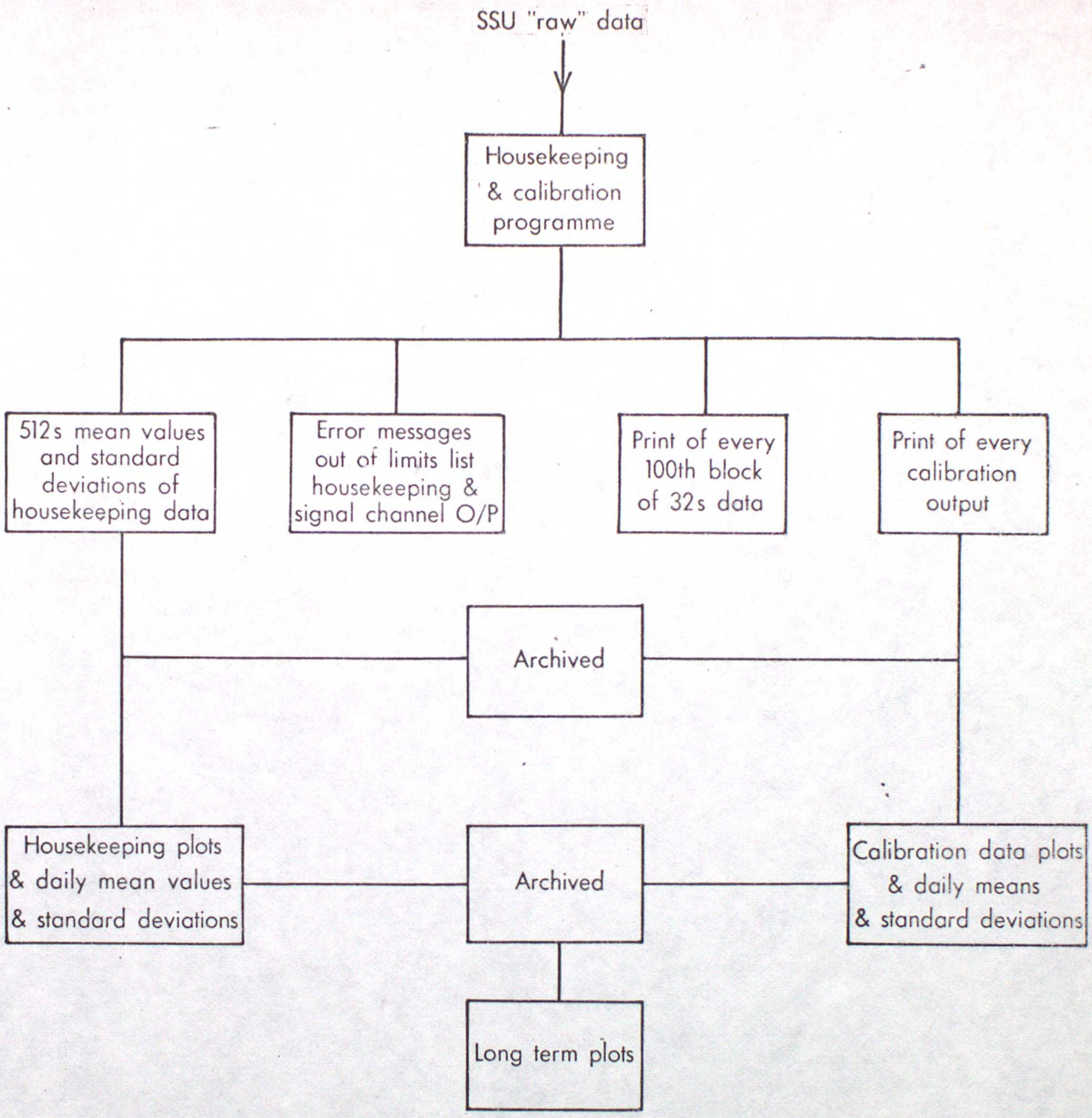

Figure 2 Data processing scheme for monitoring in-orbit performance of SSU

FIGURE 3. An example of the daily plots of some of the housekeeping monitors for TIROS -N SSU.

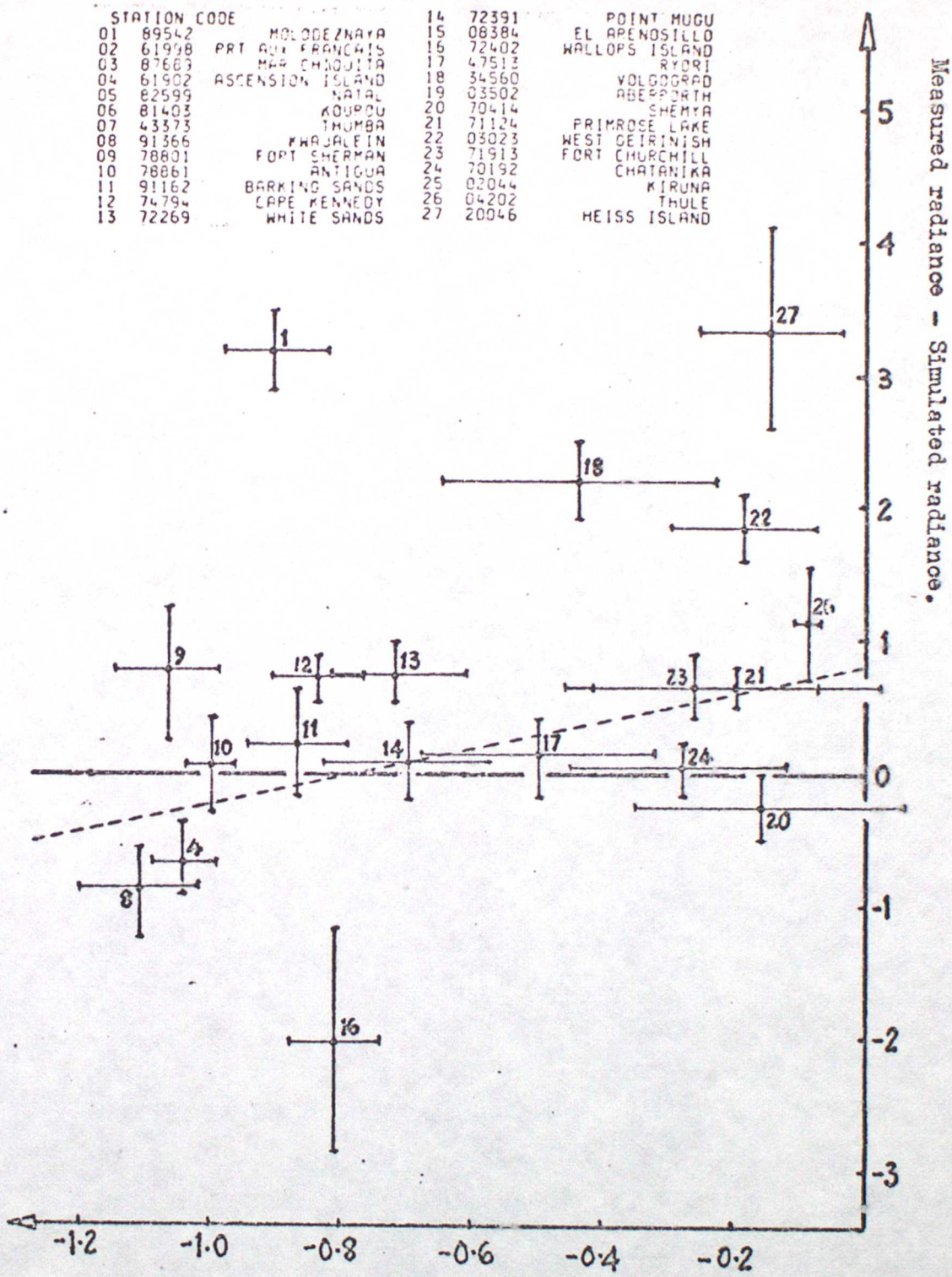

FIGURE 4. Comparison between the simulated radiance calculated from a rocket sonde temperature profile for TIROS N SSU and the satellite radiance interpolated to the rocket site; plotted as station averages identified by its station code. For channel 25.

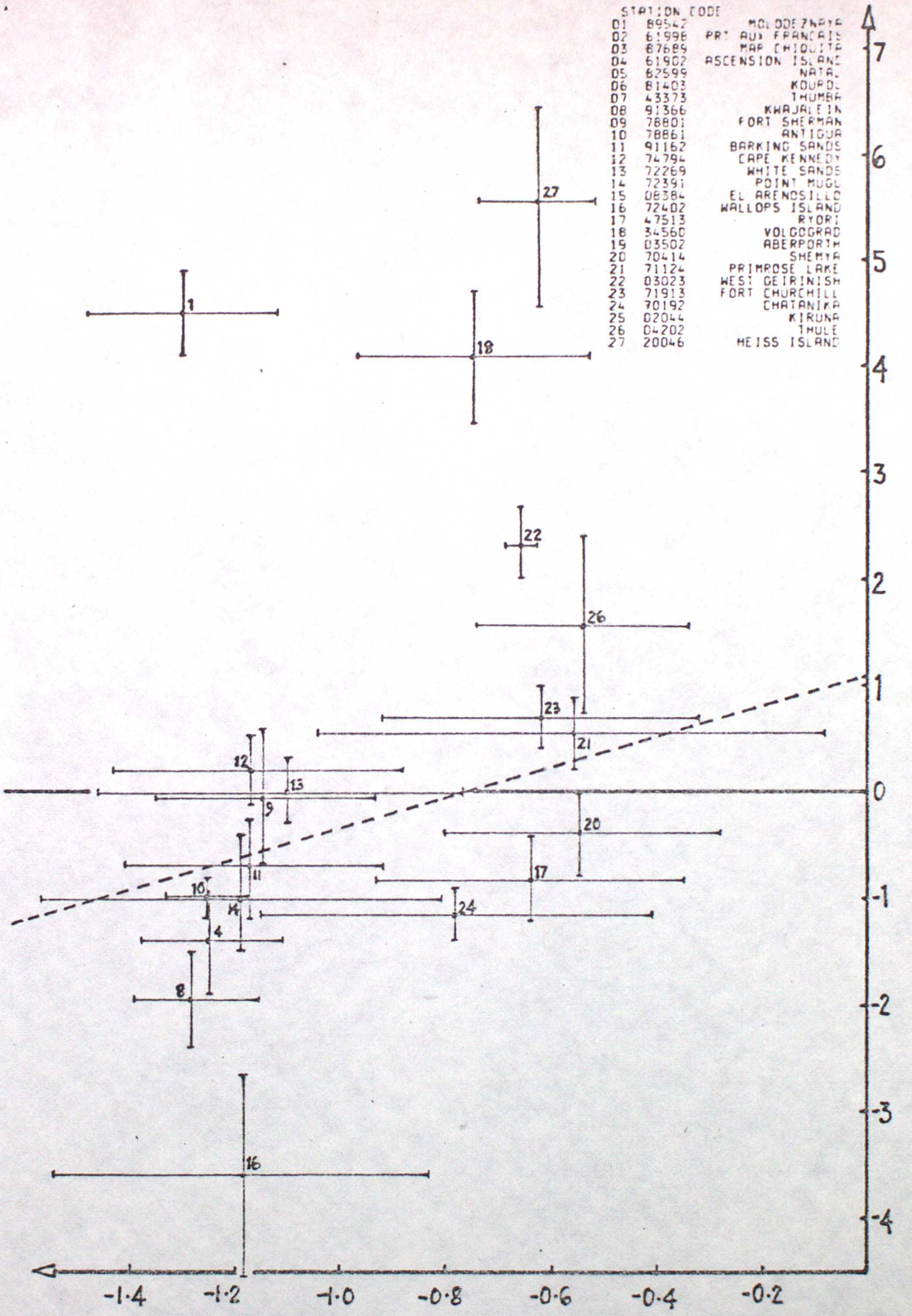

FIGURE 5. As Figure 4 except for channel 26.

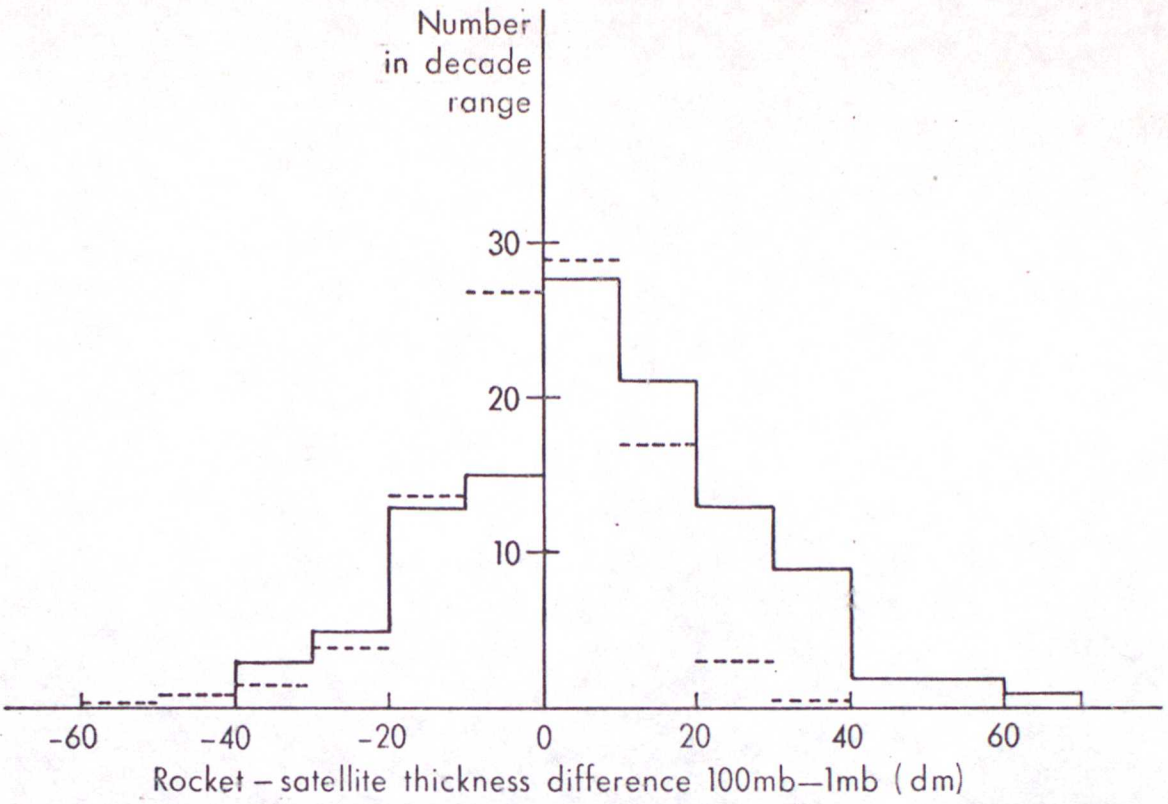

—— Tiros N collocated set

----- Basic atmosphere statistics set and simulated retrievals (scaled)

	Mean	s.d.
——	8.	19.
----	0·3	14.

Figure 6 Histogram of 100mb—1mb rocket/satellite derived thickness

Data has been screened to collocations within 125km and ± 12hr; dynamic situations, tight gradients and Russian profiles have been removed

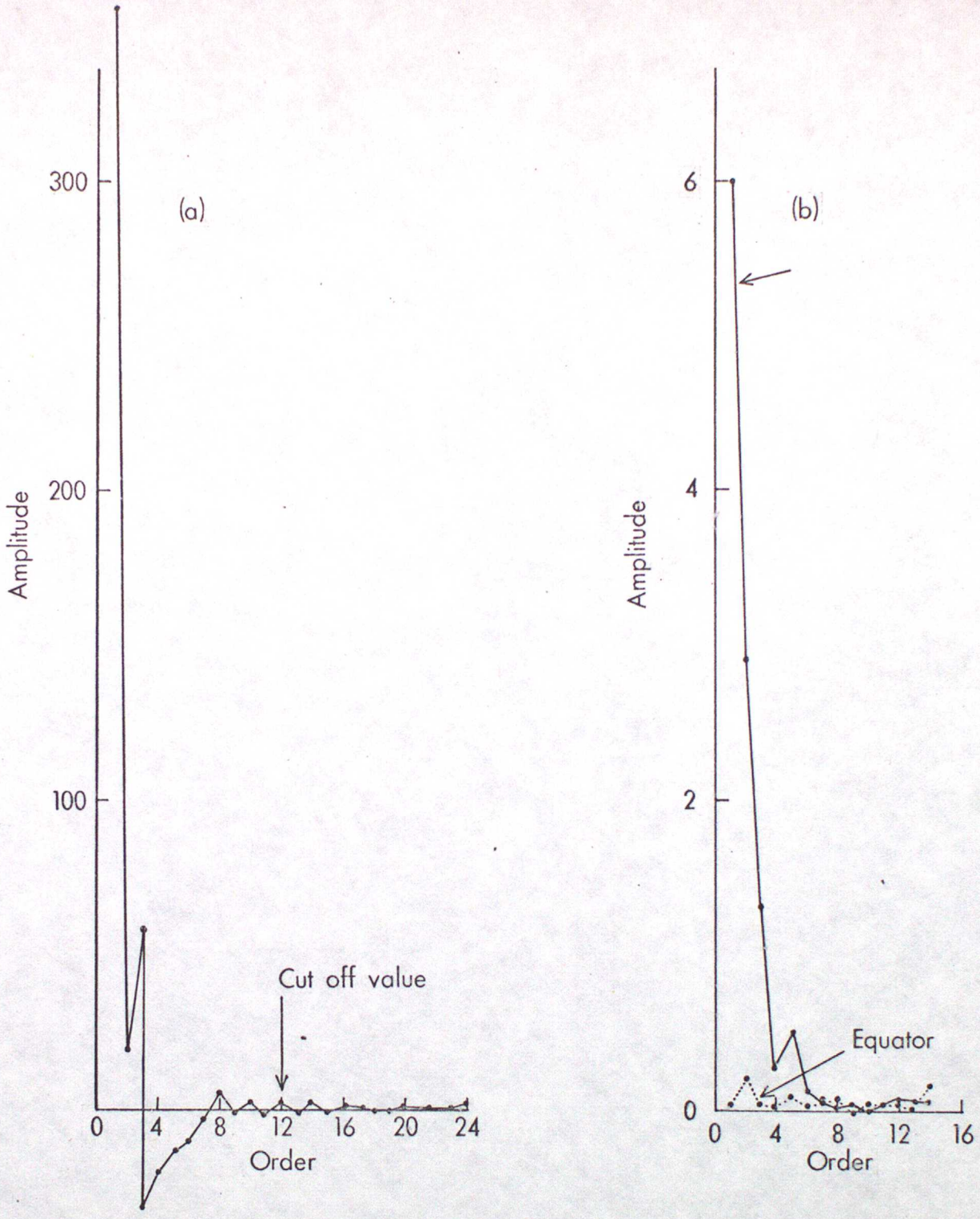

Figure 7 Example of the amplitude of the coefficients as a function of order for the orthogonal polynomials used in the analysis

(a) Polar stereographic grid (Northern channel 25 Radiance day 79004)

(b) Rectangular plots (channel 25 radiance)

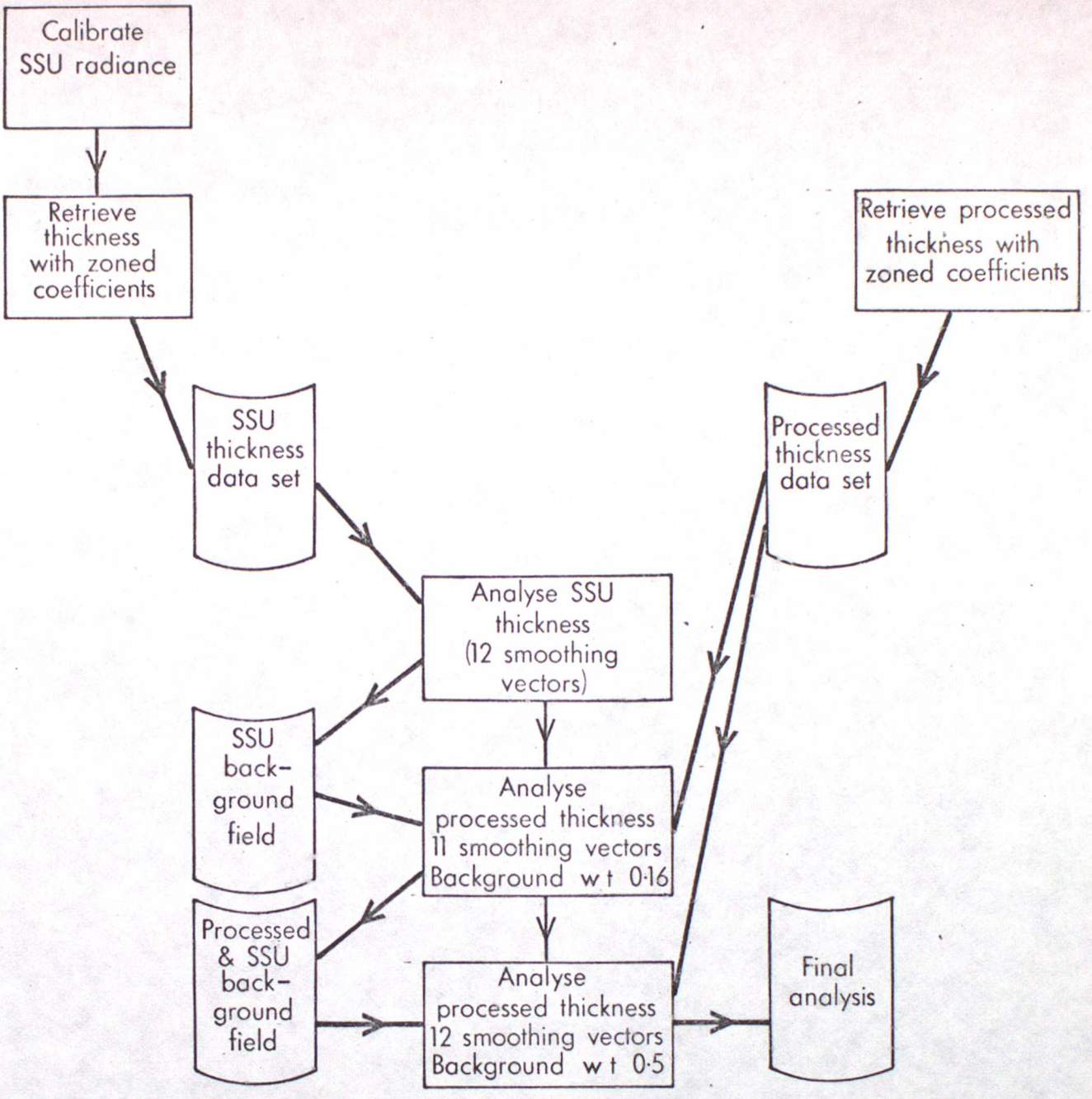

"Smoothing vector" is synonymous with "order of orthogonal polynomial used for smoothing"

Figure 8 The multiple analysis scheme

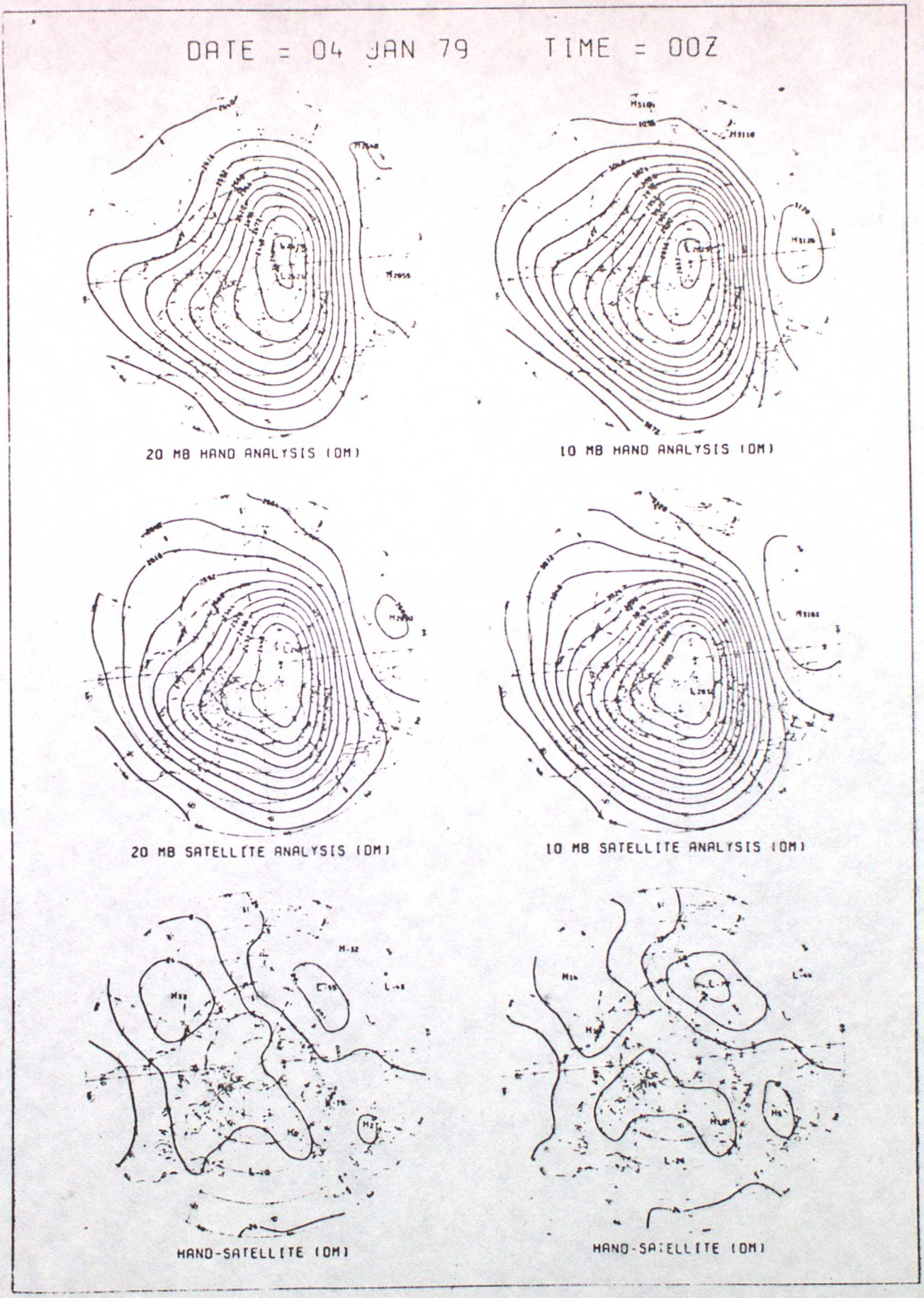

FIGURE 9 Comparisons of charts at 20 and 10 mbar produced by manual analysis of radiosonde and rocketsonde observations ('hand analysis') and by objective analysis of thickness retrievals from TIROS-N SSU radiances using un-zoned coefficients added to a conventional 100 mbar height field ('satellite analysis').

Figure 10 Tiros N simplified flow diagram

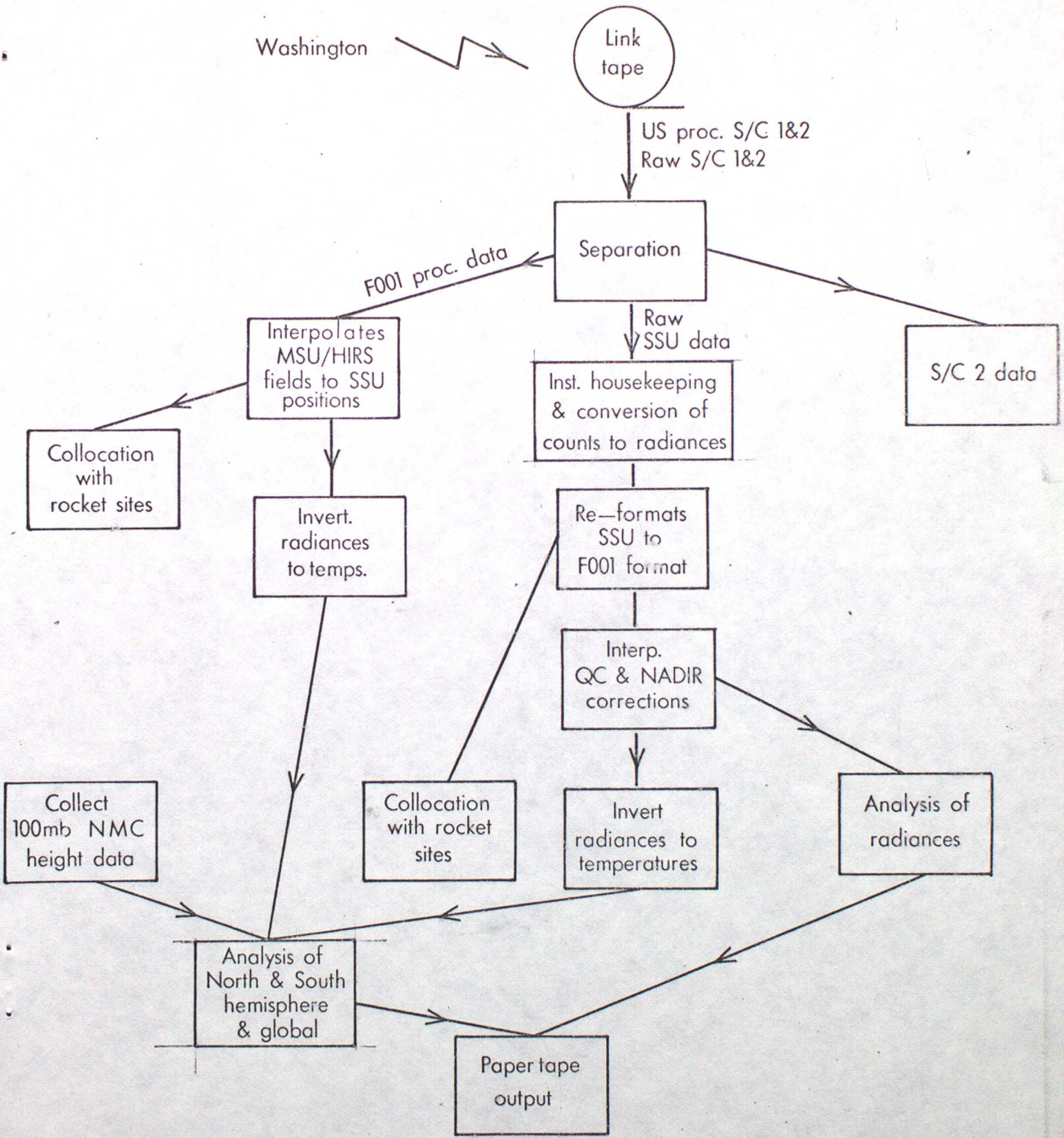

FIRURE 11(a) Data received from USA, plotted as a record of the sub-satellite position. This chart covers the period 12 hours either side of 0001 GMT on 1 July 1979, and is for TIROS-N.

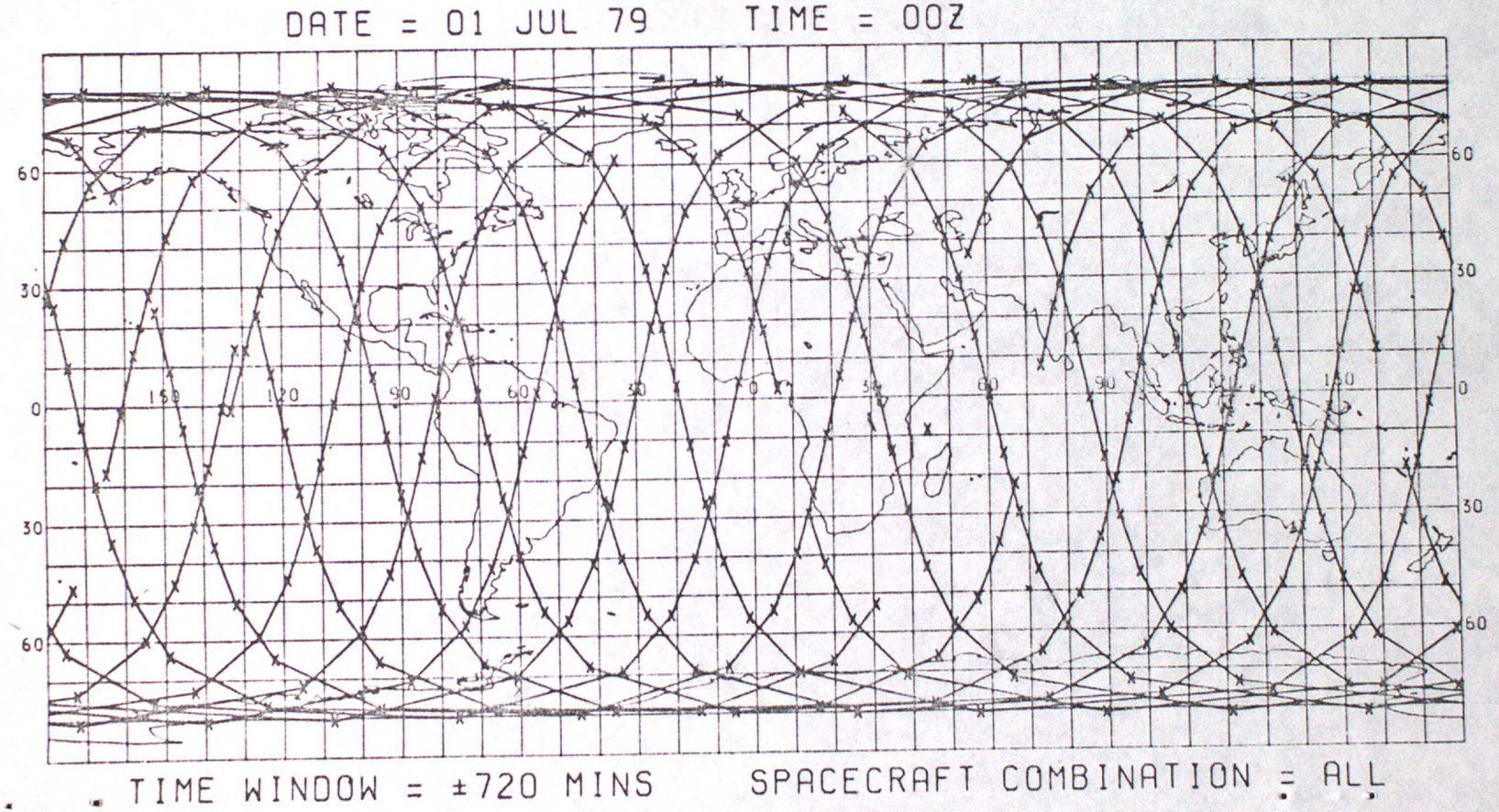

FIGURE 11(b) As Fig 11(a), except for NOAA-6. Note that data was not received from several orbits, but the SSU was only switched on during the preceeding day. Such plots highlight gaps in coverage and can thus be used to determine the confidence to be attached to features within the analyses.

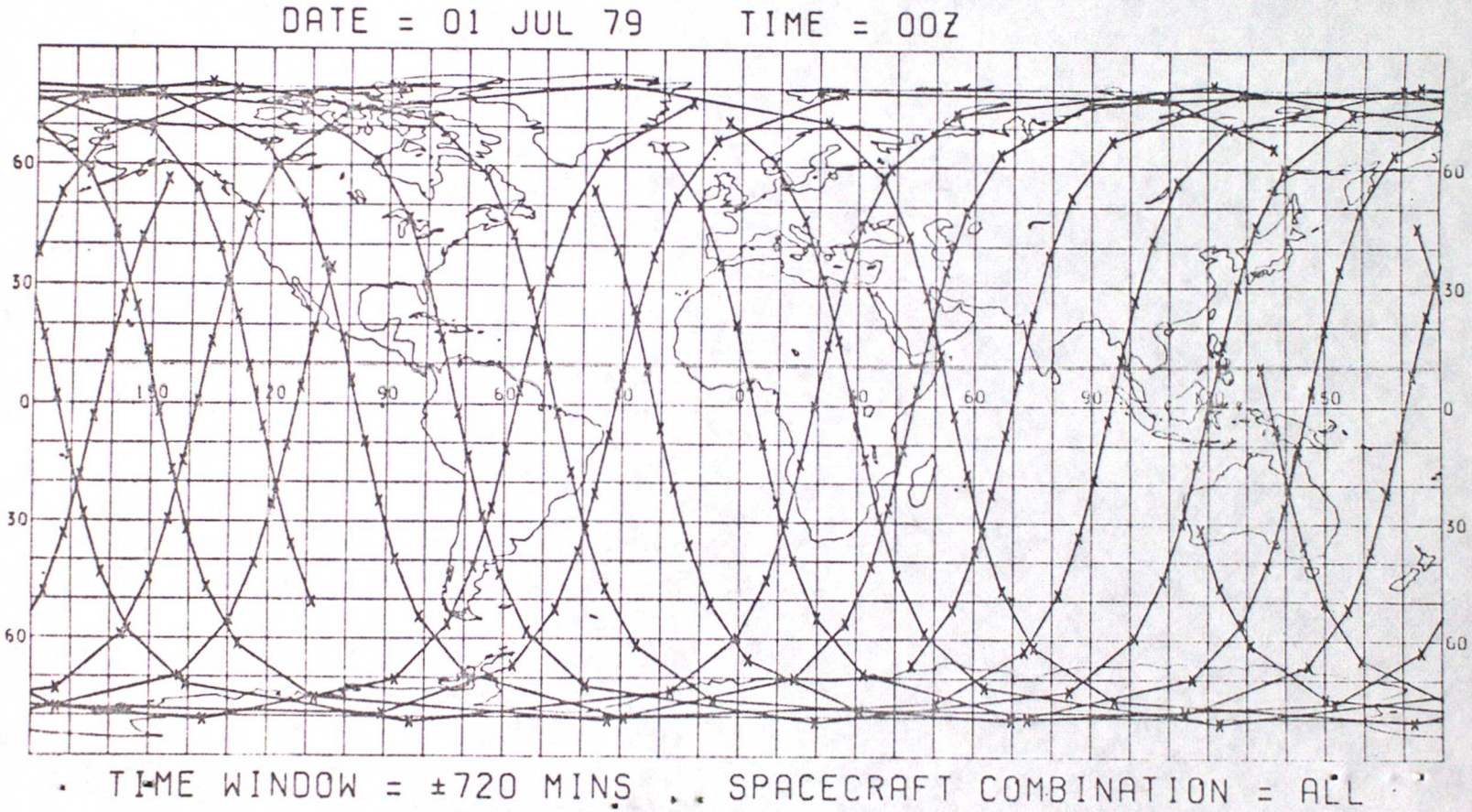

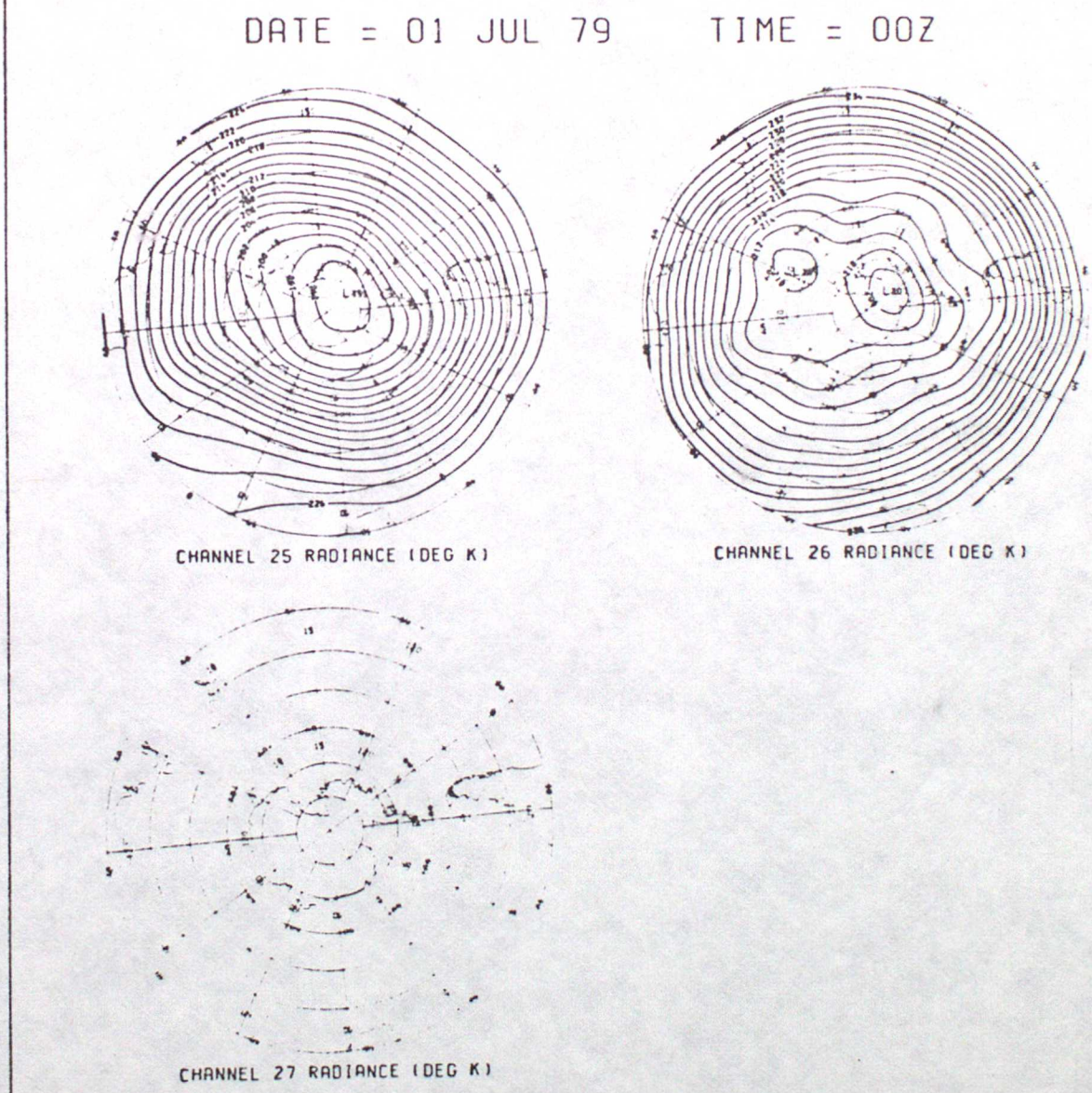

FIGURE 12(a) Objective analyses of radiances (expressed as brightness temperatures) for the southern hemisphere (latitudes 30-90°S) for the 24 hr period centred on 0001 GMT, 1 July 1979, observed by the Stratospheric Sounding Unit on TIROS-N.

DATE = 01 JUL 79 . TIME = 00Z

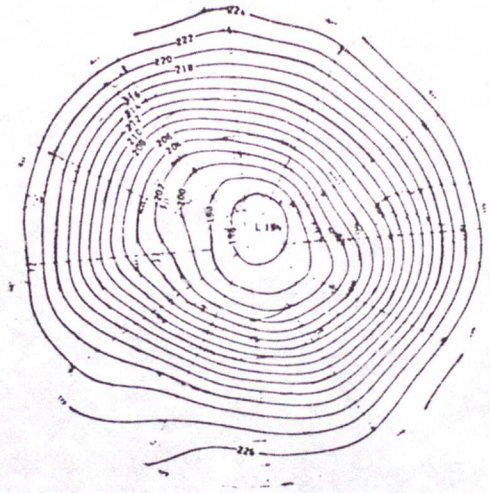

CHANNEL 25 RADIANCE (DEG K)

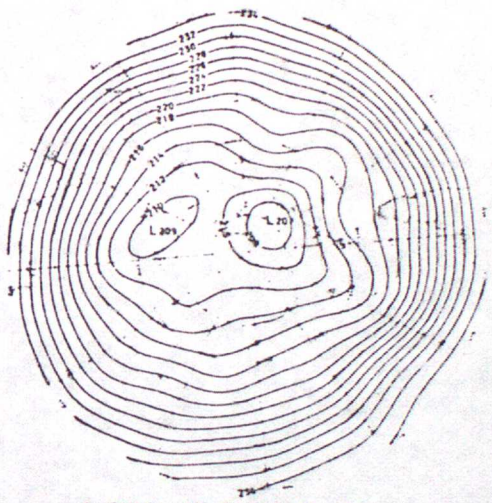

CHANNEL 26 RADIANCE (DEG K)

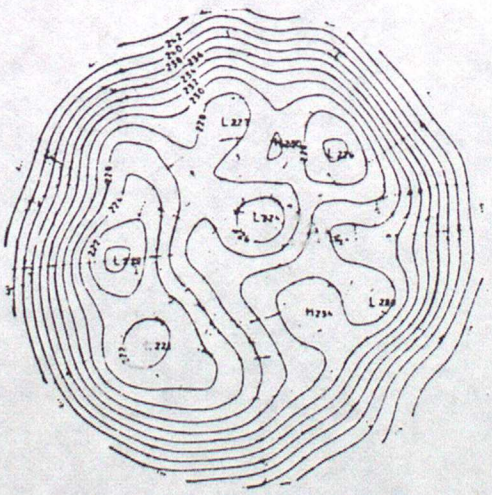

CHANNEL 27 RADIANCE (DEG K)

FIGURE 12(b) As for Figure 12(a), but using observations from the SSU on NOAA-6.

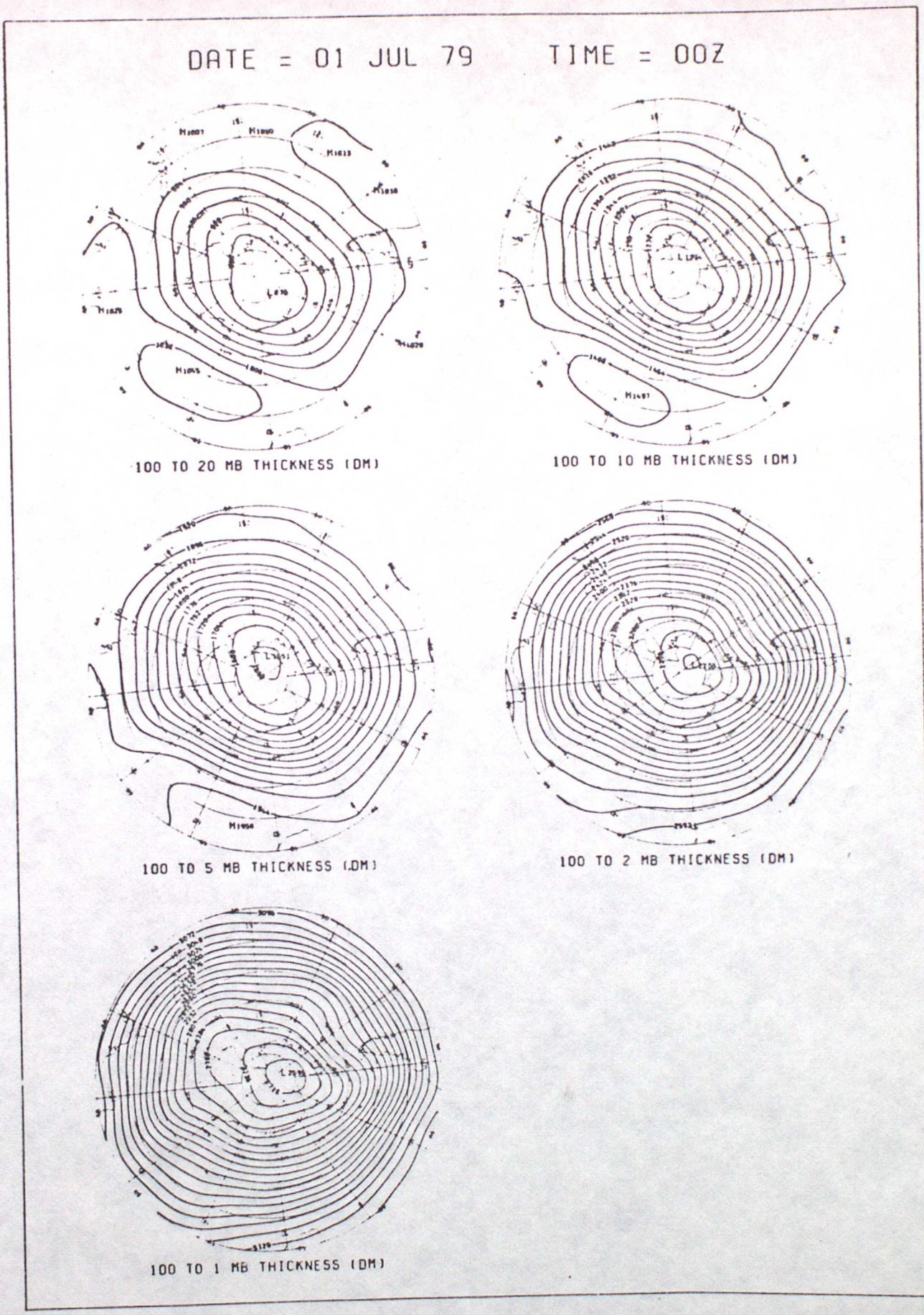

FIGURE 13(a) Objective analyses of layer thicknesses for the southern hemisphere for the 24 hr period centred on 0001 GMT, 1 July 1979, based on retrievals from "processed data" from TIROS-N, using zoned regression coefficients.

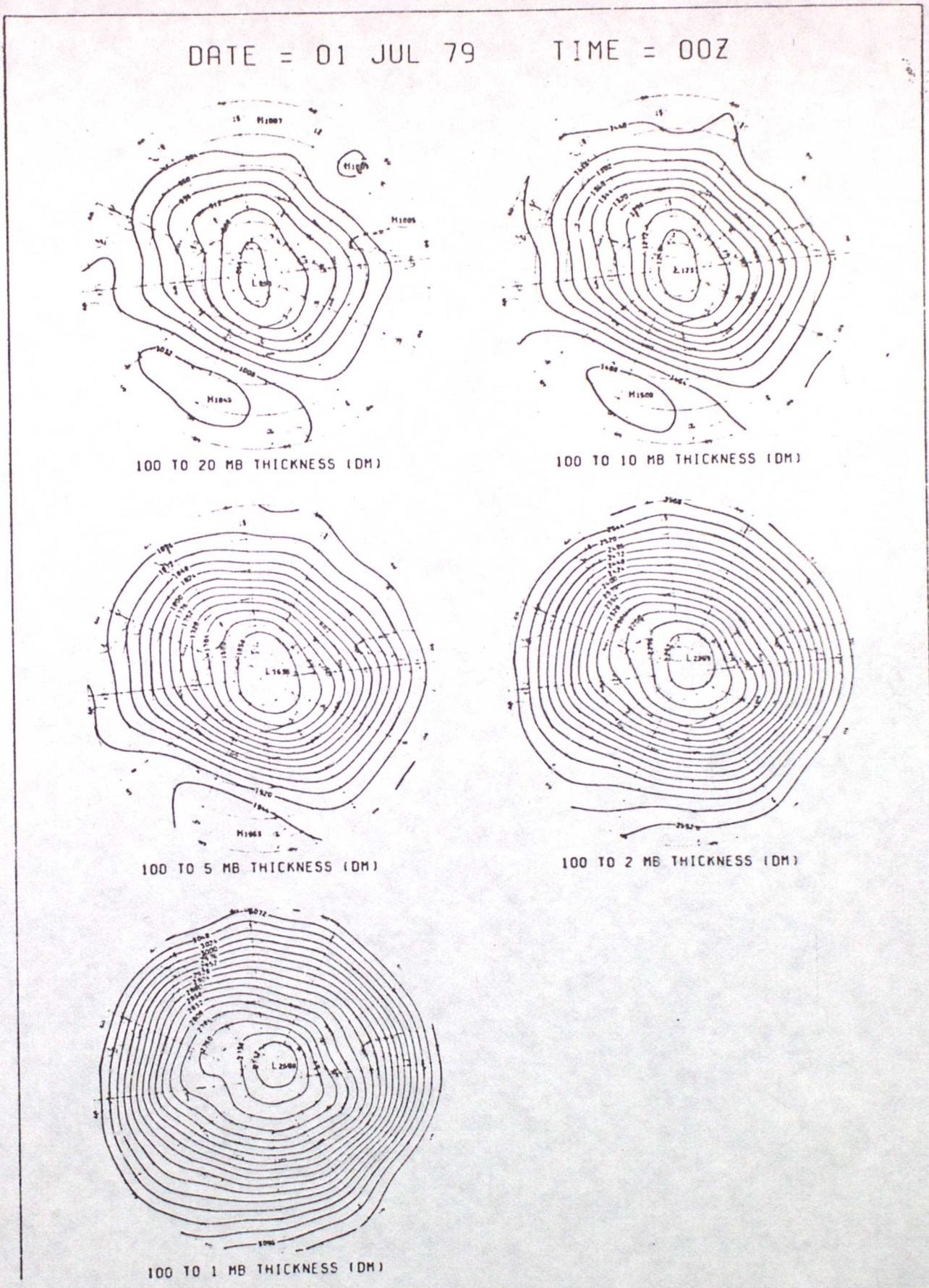

FIGURE 13(b) As for 13(a), but based on retrievals from SSU data only from NOAA-6.

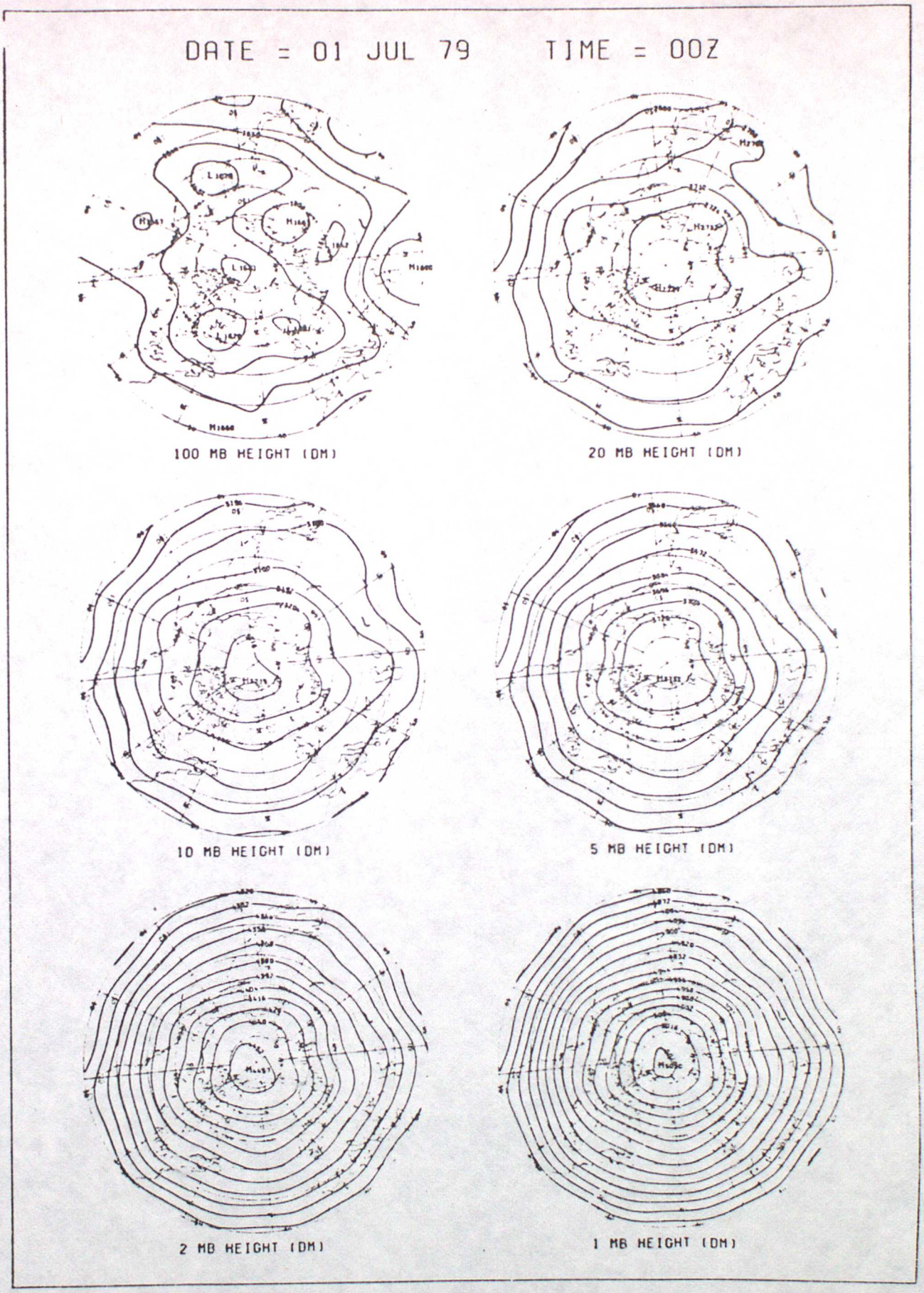

FIGURE 14 Geopotential height analyses for the northern hemisphere for 0001 GMT on 1 July 1979. The 100 mbar field is taken from NOAA/NMC global analysis. The other fields are derived from satellite-based thickness analyses relative to the 100 mbar surface. The thickness values were retrieved from "processed data" from TIROS-N.

Annex A

LIST OF TIROS-N/NOAA-6 DATA AND PRODUCTS, AUGUST 1979

PRODUCT	AVAILABILITY		SOURCE/FORMAT			CHART TYPE (where appropriate)			REMARKS
	ARCHIVE	CHART	RAW	F.O.V	ANALYSIS	POLAR N HEM	STEREO S HEM	RECTANGULAR TROPICAL	
SSU raw data	✓		✓						
SSU radiances, earth located and calibrated	✓			✓					
SSU radiances (calibrated in-house)	✓	✓			✓	✓	✓	✓	Plotted as brightness temperature
Processed radiances from HIRS, MSU and SSU	✓			✓					
Retrieved thicknesses: 100 mbar to 20, 10, 5, 2 and 1 mbar	✓			✓					
Retrieved thicknesses: 100 mbar to 20, 10, 5, 2 and 1 mbar	✓	✓			✓	✓	✓	✓	Based on TIROS-N processed data and NOAA-6 SSU data
Heights: 100, 20, 10, 5, 2, 1 mbar	✓	✓			✓	✓	(✓)	(✓)	Heights archived with thicknesses. Heights will eventually be global
Winds: 100, 20, 10, 5, 2 and 1 mbar		✓				✓	(✓)		Gradient winds derived from height fields
Coverage obtained for SSU radiances		✓		✓				✓	Used to gauge reliability of analysed charts
Coverage obtained for processed radiances		✓		✓				✓	Used to gauge reliability of TIROS-N multiple analysis
Instrument Housekeeping	✓	✓	✓						

PRODUCT	AVAILABILITY		SOURCE/FORMAT			CHART TYPE (where appropriate)			REMARKS
	ARCHIVE	CHART	RAW	F.O.V	ANALYSIS	POLAR N HEM	STEREO S HEM	RECTANG-ULAR TROPICAL	
Radiometric calibration values	✓	✓	✓						
SSU radiances co-located with rocket sites	✓			✓					
Processed radiances co-located with rocket sites	✓			✓					
Analysed heights, winds and radiances at rocket sites	✓								Site values extracted objectively from analysed retrievals